Implementation of a Body Force Model into OVERFLOW for Propulsor Simulations*

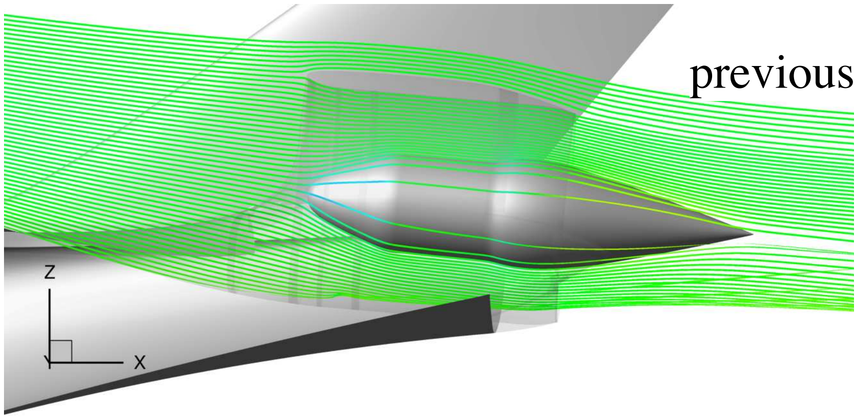

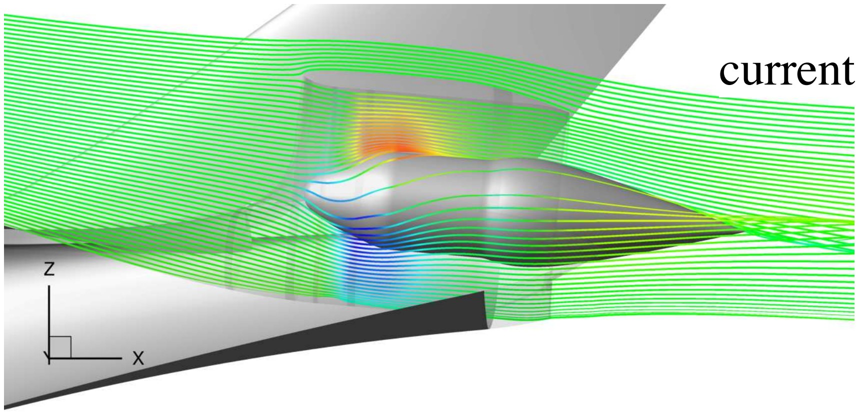

H. Doğuş Akaydın
Senior Research Scientist/Engineer
Science and Technology Corporation
at NASA Ames Research Center

Shishir A. Pandya
Aerospace Engineer
NASA Ames Research Center

*Paper: AIAA-2017-3572

Applied Modeling and Simulation Seminar – 19 October 2017
Advanced Supercomputing Division, Computational Aerosciences Branch
NASA Ames Research Center

NASA is actively sponsoring research and development of cleaner, less noisy and more efficient transport aircraft

v2016.1

TECHNOLOGY BENEFITS	TECHNOLOGY GENERATIONS (Technology Readiness Level = 5-6)		
	Near Term 2015-2025	**Mid Term** 2025-2035	**Far Term** beyond 2035
Noise (cum below Stage 4)	**22 - 32 dB**	**32 - 42 dB**	**42 - 52 dB**
LTO NOx Emissions (below CAEP 6)	**70 - 75%**	**80%**	**> 80%**
Cruise NOx Emissions (rel. to 2005 best in class)	**65 - 70%**	**80%**	**> 80%**
Aircraft Fuel/Energy Consumption (rel. to 2005 best in class)	**40 - 50%**	**50 - 60%**	**60 - 80%**

An ~~over~~view of the state of the art: plan

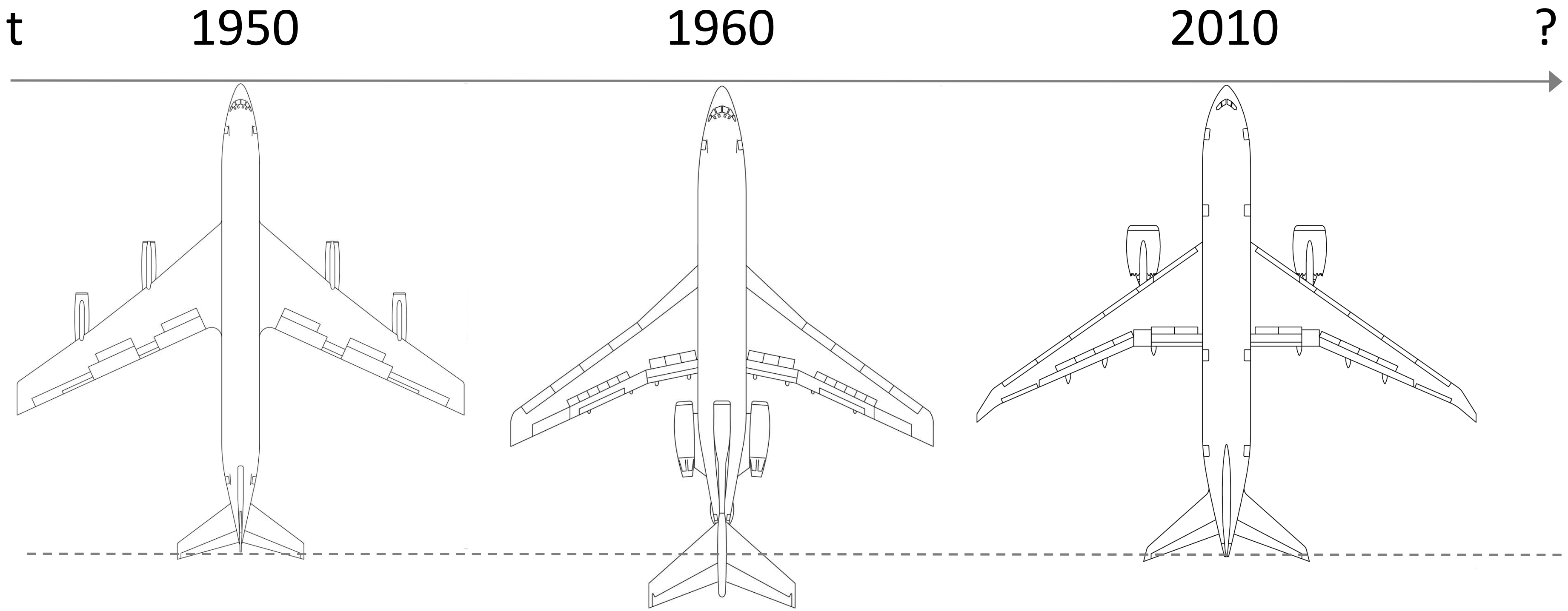

Progress in commercial transport aircraft has been driven mainly by

- Engines (became more efficient, more powerful and more reliable)
- Composite structures (became more reliable)
- Control surfaces and avionics (became more sophisticated)

Airframe integration, however, lagged: Thin-tube fuselages and wing-mounted engines are still the state of the art.

One of the concepts: The D8 "Double Bubble" Aircraft

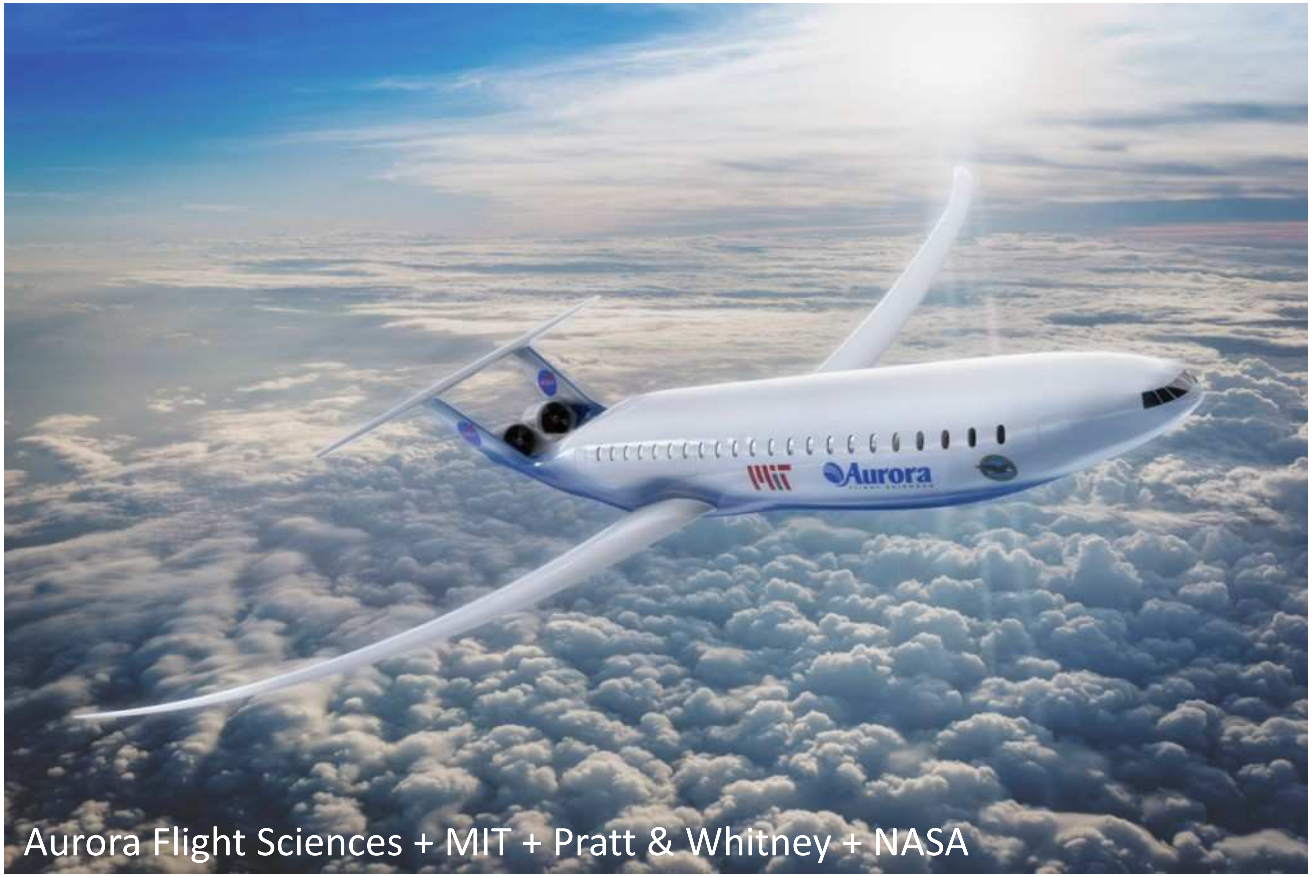

MIT: Lead the research, design the aircraft, perform wind tunnel tests
Aurora Flight Sciences: Build wind tunnel models and flight demonstrators
Pratt & Whitney: Develop the engines
NASA: Sponsor the project, provide wind tunnel and computer time for advanced analysis

How does Boundary Layer Ingestion work?

Instead of accelerating freestream, the propulsors accelerate the fluid that was decelerated by the body. This reduces the total form drag.

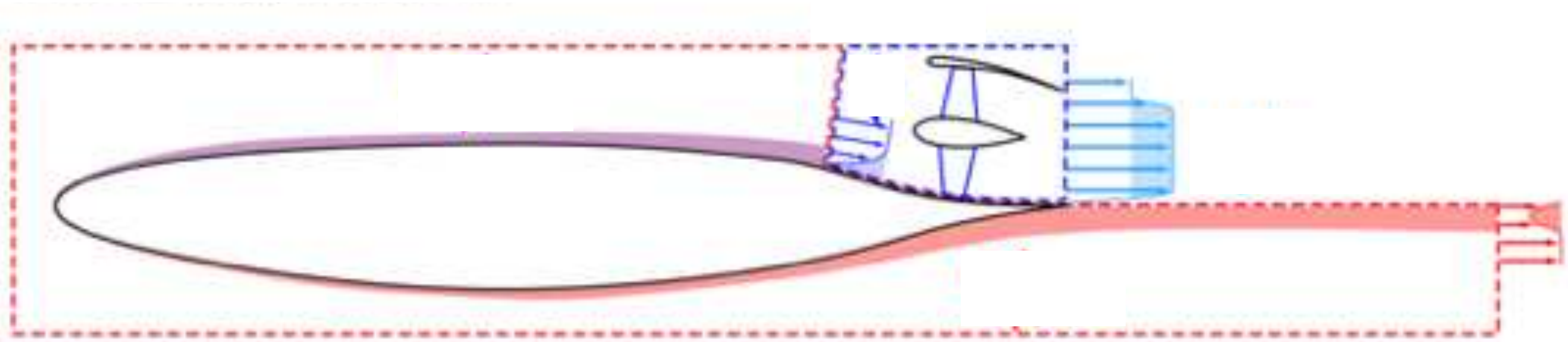

Drela, *Power Balance in Aerodynamic Flows*, 2009, AIAA Journal 47(7)
Drela, *Development of the D8 Transport Configuration*, 2011, AIAA-2011-3970
Uranga *et al.*, *Preliminary Experimental Assessment of the Boundary Layer Ingestion Benefit for the D8 Aircraft*, AIAA-2014-0906

>30% reduction in fuel burn due to the synergistic *integration* of airframe components

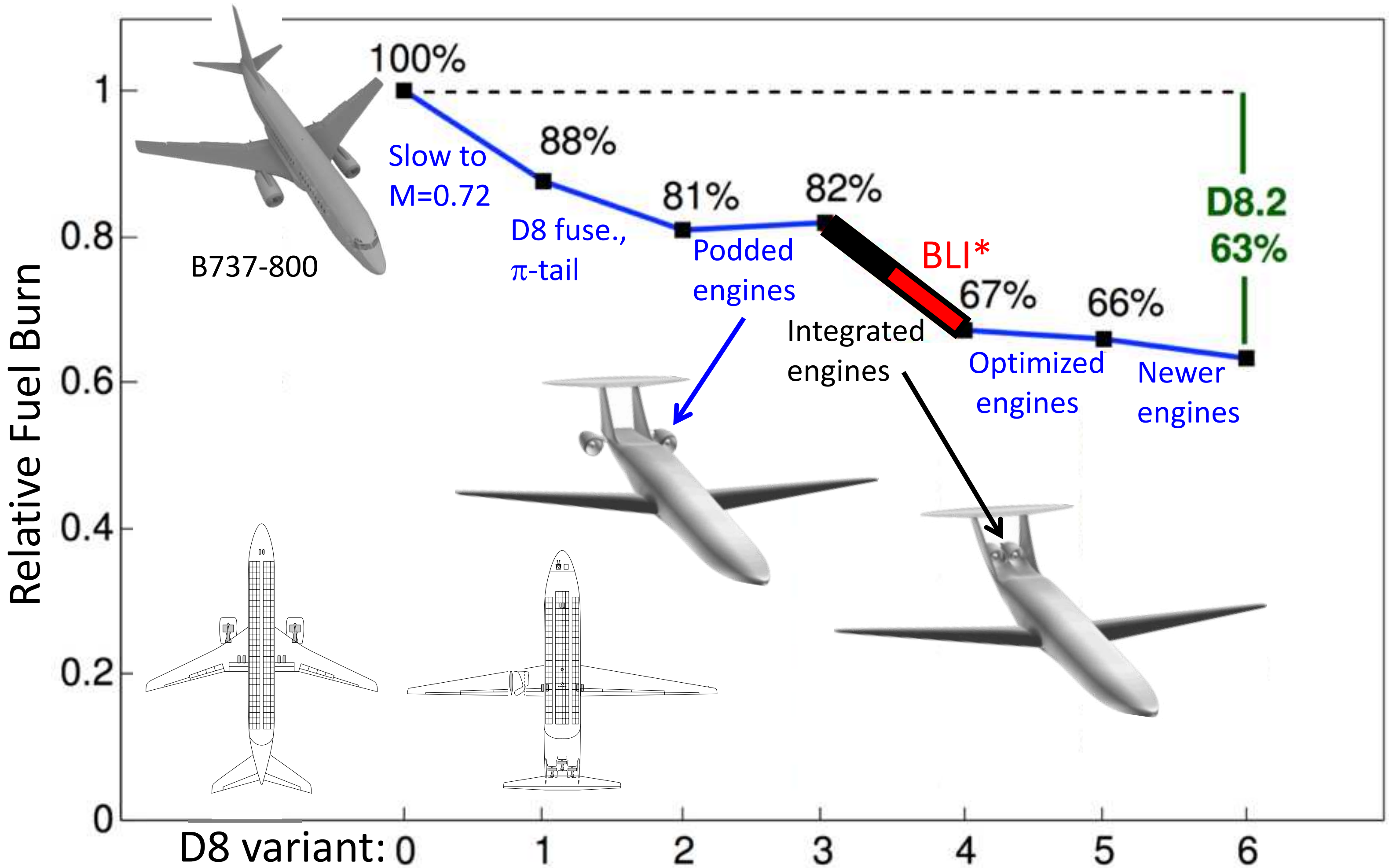

*BLI: Boundary Layer Ingestion

Greitzer *et al.*, *N+3 Aircraft Concept Designs and Trade Studies. Volume 1*, 2010, NASA CR-2010-216794/VOL1

Uranga *et al.*, *Preliminary Experimental Assessment of the Boundary Layer Ingestion Benefit for the D8 Aircraft*, AIAA-2014-0906

The D8 aircraft in wind tunnel

Tests 14x22ft Wind Tunnel at NASA Langley Research Center

Uranga *et al.*, *Preliminary Experimental Assessment of the Boundary Layer Ingestion Benefit for the D8 Aircraft*, AIAA-2014-0906

CFD (Computational Fluid Dynamics) simulations of the model in the wind tunnel

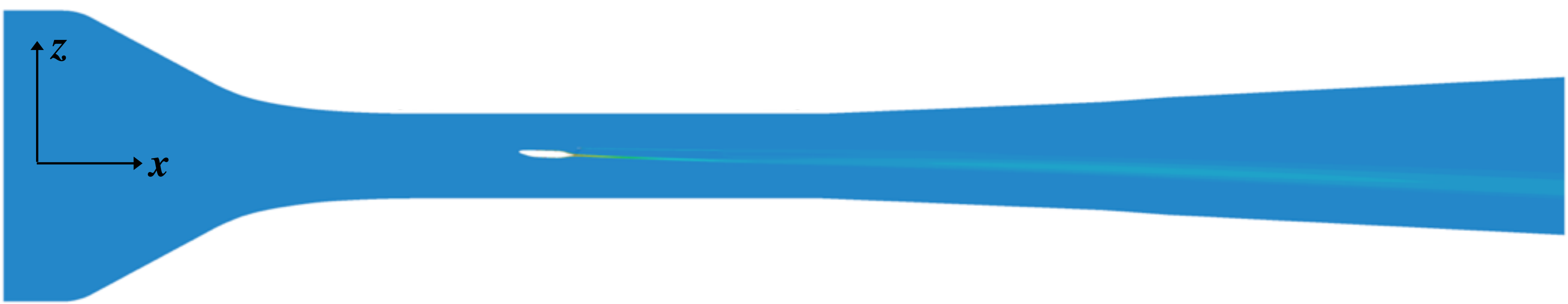

Pandya, *External Aerodynamics Simulations for the MIT D8 “Double-Bubble” Aircraft Design*, 2012, ICCFD7-4304

Evidence of BLI benefit through CFD and wind tunnel tests

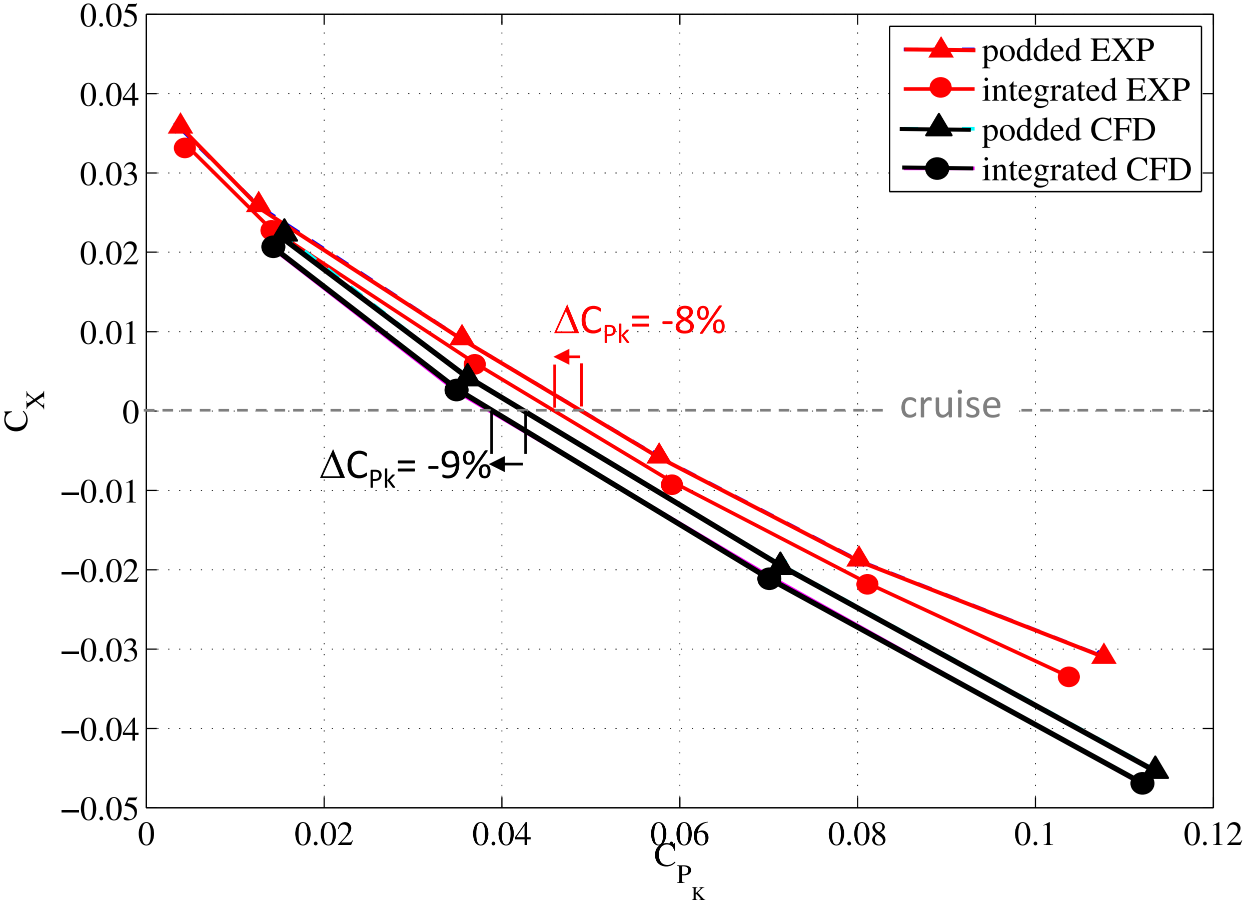

Wind tunnel tests show an 8% ± 0.7% reduction in power to sustain cruise.

CFD predicts a 9% reduction.

Greitzer *et al.*, *Aircraft and Technology Concepts for an N+3 Subsonic Transport – Phase 2. Final Review,* Dec. 2014

Uranga *et al.*, *Preliminary Experimental Assessment of the Boundary Layer Ingestion Benefit for the D8 Aircraft*, AIAA-2014-0906

Pandya *et al.*, *Computational Assessment of the Boundary Layer Ingesting Nacelle Design of the D8 Aircraft*, AIAA-2014-0907

The application: Boundary Layer Ingestion (BLI) on D8 aircraft

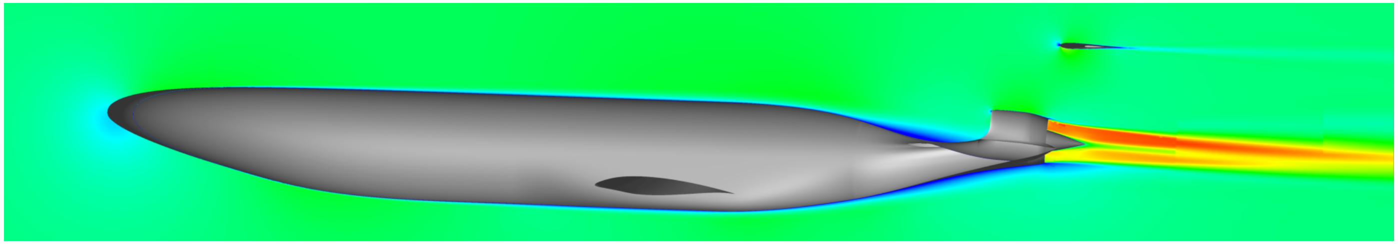

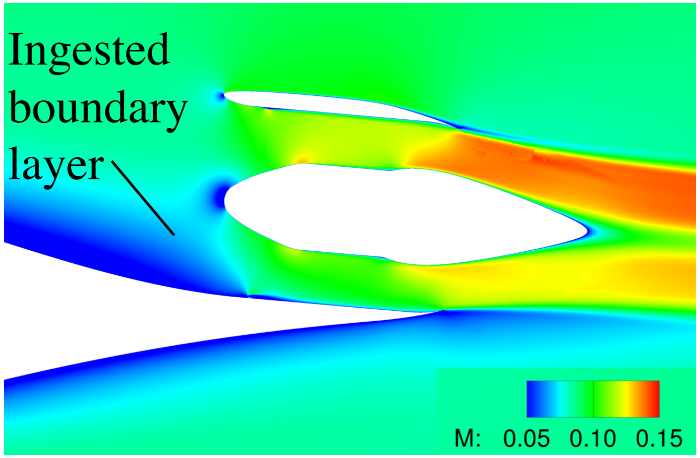

The application: Boundary Layer Ingestion (BLI) on D8 aircraft

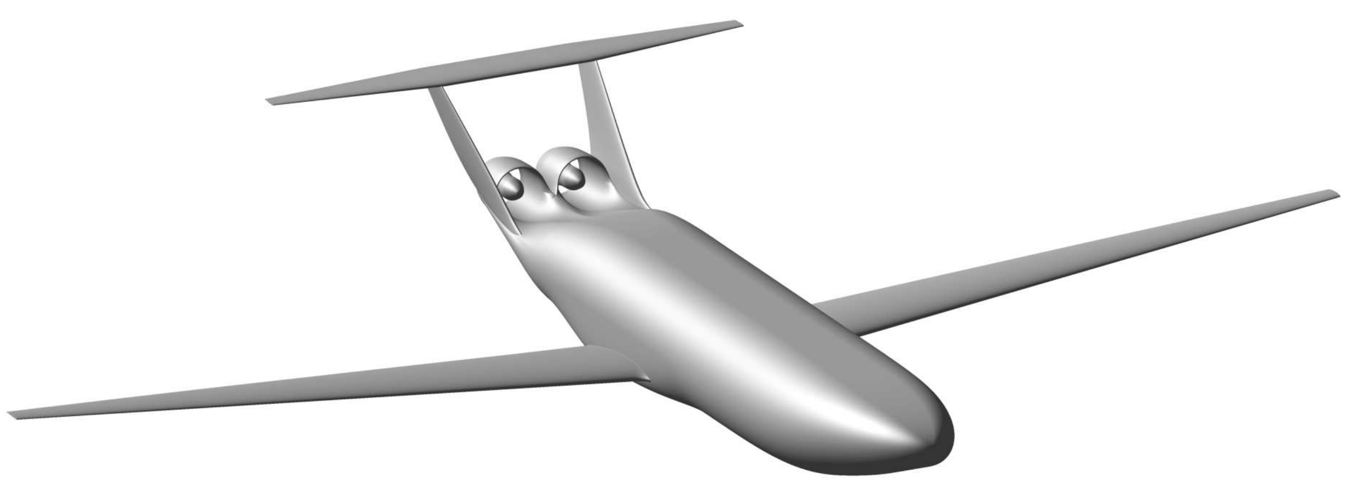

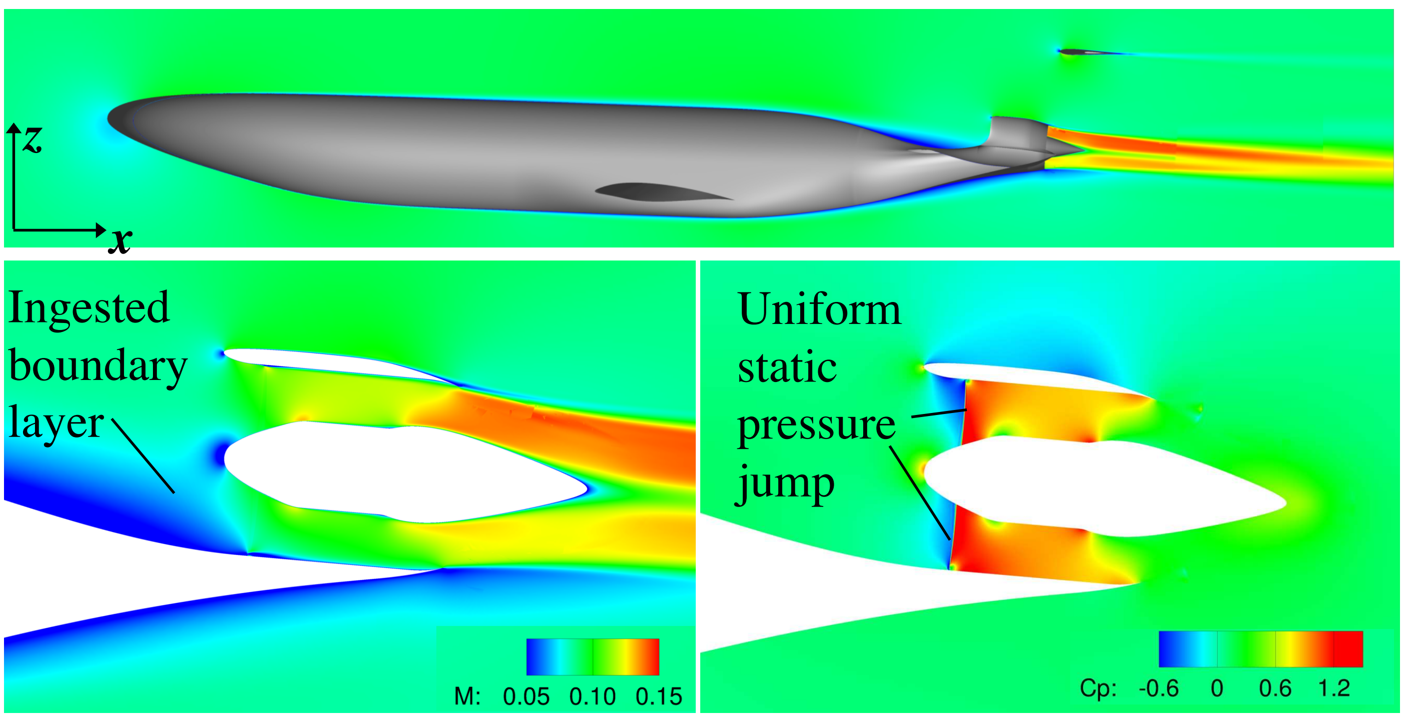

Previous method:
Uniform static pressure jump

$$p_{\text{avg}} = 0.5(p_J + p_{J+1})$$
$$p_J = p_{\text{avg}} - 0.5\Delta p$$
$$p_{J+1} = p_{\text{avg}} + 0.5\Delta p$$

(No jump applied on ρ, T)

Literature on Propulsor Modeling

Variants of actuator disk or blade element models

Helicopter rotors & wind turbine applications

Fejtek and Roberts [1992]
Zori and Rajagopalan [1995]
Chaffin and Berry [1997] --> Two versions are already in Overflow
O'Brien and Smith [2005]
… many others.

Literature on Propulsor Modeling

Variants of actuator disk or blade element models

Helicopter rotors & wind turbine applications

Fejtek and Roberts [1992]
Zori and Rajagopalan [1995]
Chaffin and Berry [1997] --> Two versions are already in Overflow
O'Brien and Smith [2005]
… many others.

Turbomachine applications

Joo and Hynes [1997]
Kim et al. [1999]
...

Literature on Propulsor Modeling

Variants of actuator disk or blade element models

Helicopter rotors & wind turbine applications

Fejtek and Roberts [1992]
Zori and Rajagopalan [1995]
Chaffin and Berry [1997] --> Two versions are already in Overflow
O'Brien and Smith [2005]
… many others.

Turbomachine applications

Joo and Hynes [1997]
Kim et al. [1999]
...

A particular series of "body-force" approaches for turbomachines

Marble [1964]
...
Gong et al. [1998]
Defoe and Spakovszky [2013]
Peters et al. [2014]
Hall et al. [2017]

The implemented body force model by Hall et al.

$$\nabla \cdot (\rho \mathbf{V}) = 0$$

$$\mathbf{V} \cdot \nabla \mathbf{V} + \frac{\nabla p}{\rho} = \mathbf{f}$$

$$\mathbf{V} \cdot \nabla h_t = \mathbf{V} \cdot \mathbf{f} + \dot{e}$$

Hall et al. “Analysis of Fan Stage Conceptual Design Attributes for Boundary Layer Ingestion”, 2017, ASME J. Turbomach.

The implemented body force model by Hall et al.

$$\nabla \cdot (\rho \mathbf{V}) = 0$$

$$\mathbf{V} \cdot \nabla \mathbf{V} + \frac{\nabla p}{\rho} = \mathbf{f}$$

$$\mathbf{V} \cdot \nabla h_t = \mathbf{V} \cdot \mathbf{f} + \dot{e}$$

$$f = \frac{2\pi\delta(\frac{1}{2}|\mathbf{W}|^2)}{\frac{2\pi r}{B}|n_\theta|}$$

Hall et al. "Analysis of Fan Stage Conceptual Design Attributes for Boundary Layer Ingestion", 2017, ASME J. Turbomach.

The implemented body force model by Hall et al.

$$\nabla \cdot (\rho \mathbf{V}) = 0$$

$$\mathbf{V} \cdot \nabla \mathbf{V} + \frac{\nabla p}{\rho} = \mathbf{f}$$

$$\mathbf{V} \cdot \nabla h_t = \mathbf{V} \cdot \mathbf{f} + \dot{e}$$

$$f = \frac{2\pi\delta(\frac{1}{2}|\mathbf{W}|^2)}{\frac{2\pi r}{B}|n_\theta|}$$

$$\dot{e} = T \cdot \mathbf{V}\nabla s = -\mathbf{W} \cdot \mathbf{f}$$

Hall et al. “Analysis of Fan Stage Conceptual Design Attributes for Boundary Layer Ingestion”, 2017, ASME J. Turbomach.

The implemented body force model by Hall et al.

$$\nabla \cdot (\rho \mathbf{V}) = 0$$

$$\mathbf{V} \cdot \nabla \mathbf{V} + \frac{\nabla p}{\rho} = \mathbf{f}$$

$$\mathbf{V} \cdot \nabla h_t = \mathbf{V} \cdot \mathbf{f} + \dot{e}$$

$$f = \frac{2\pi\delta(\frac{1}{2}|\mathbf{W}|^2)}{\frac{2\pi r}{B}|n_\theta|}$$

$$\dot{e} = T \cdot \mathbf{V}\nabla s = -\mathbf{W} \cdot \mathbf{f}$$

$$\mathbf{W} \cdot \mathbf{f} = 0 \text{ (Isentropic flow turning)}$$

Hall et al. "Analysis of Fan Stage Conceptual Design Attributes for Boundary Layer Ingestion", 2017, ASME J. Turbomach.

Implementation of the body force model

1. Import:

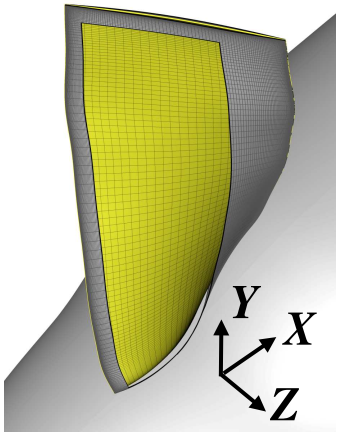

Import the surface definition of one of the blades

Implementation of the body force model

1. Import: 2. Extract:

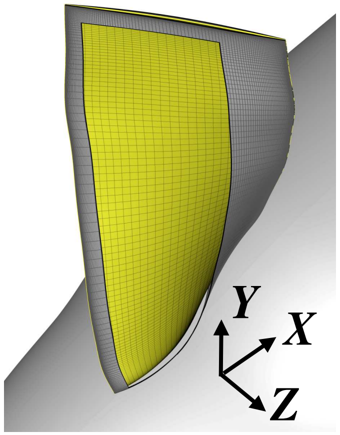

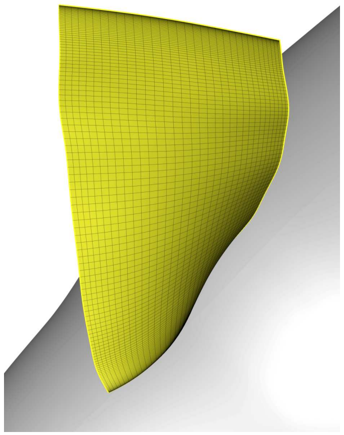

Extract the camber surface of the blade

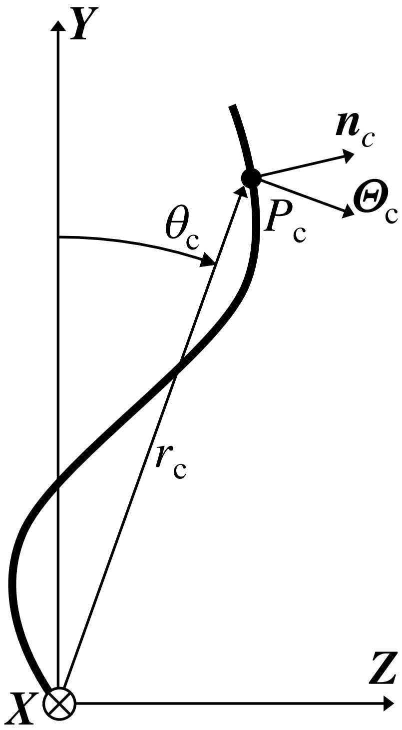

Implementation of the body force model

1. Import 2. Extract: 3. Flatten:

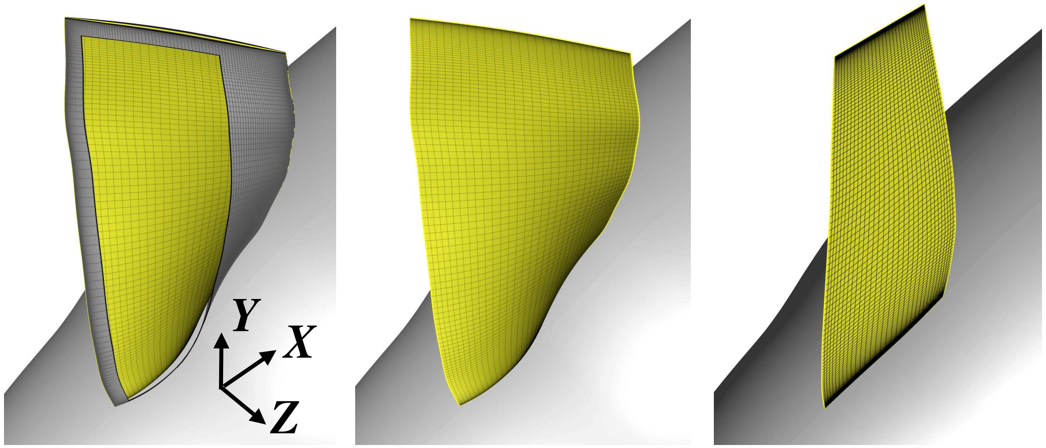

Flatten the camber surface on Z=0 plane

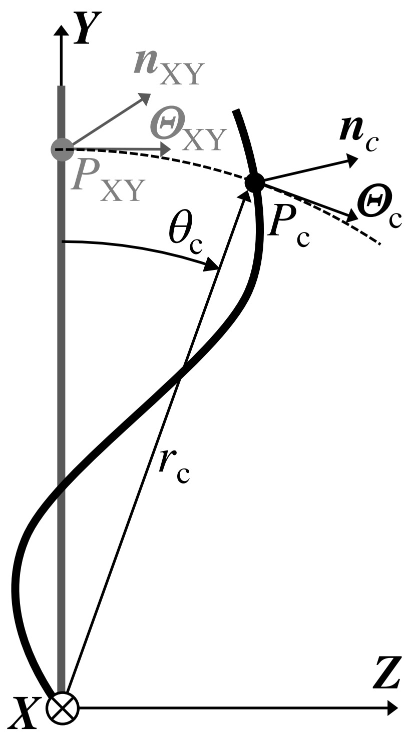

Implementation of the body force model

1. Import 2. Extract: 3. Flatten: 4. Extend:

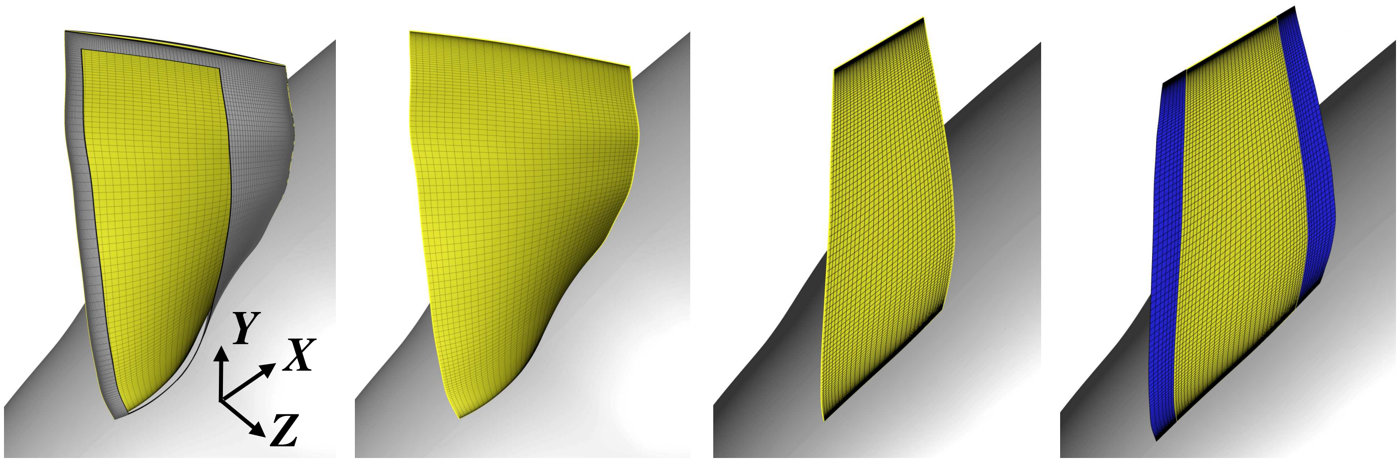

Extend for a proper overlap with neighboring grids

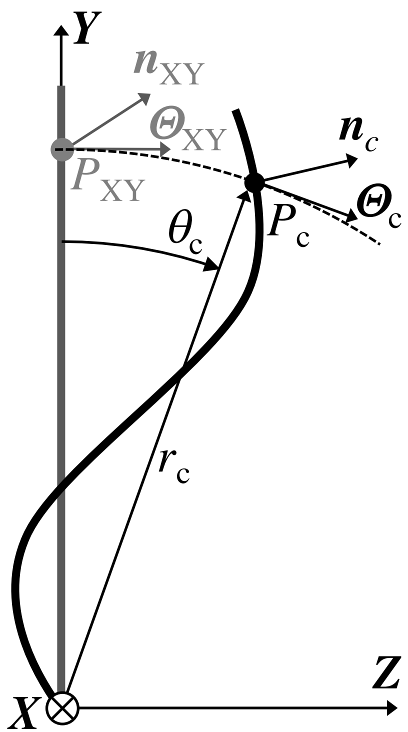

Implementation of the body force model

1. Import

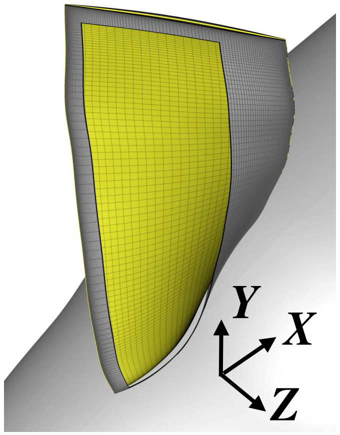

2. Extract:

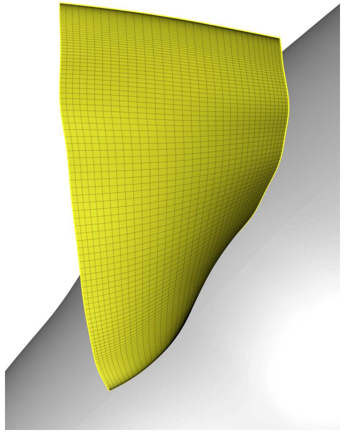

3. Flatten:

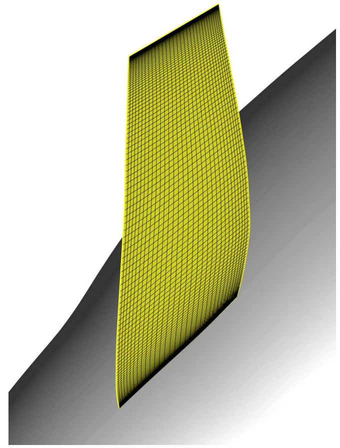

4. Extend:

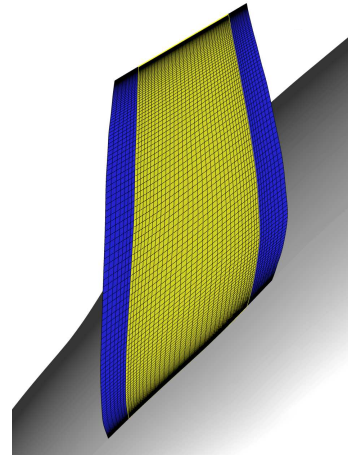

5. Revolve:

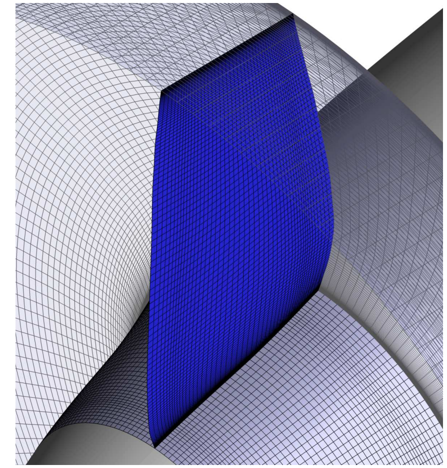

Revolve that to make an axisymmetric volume grid

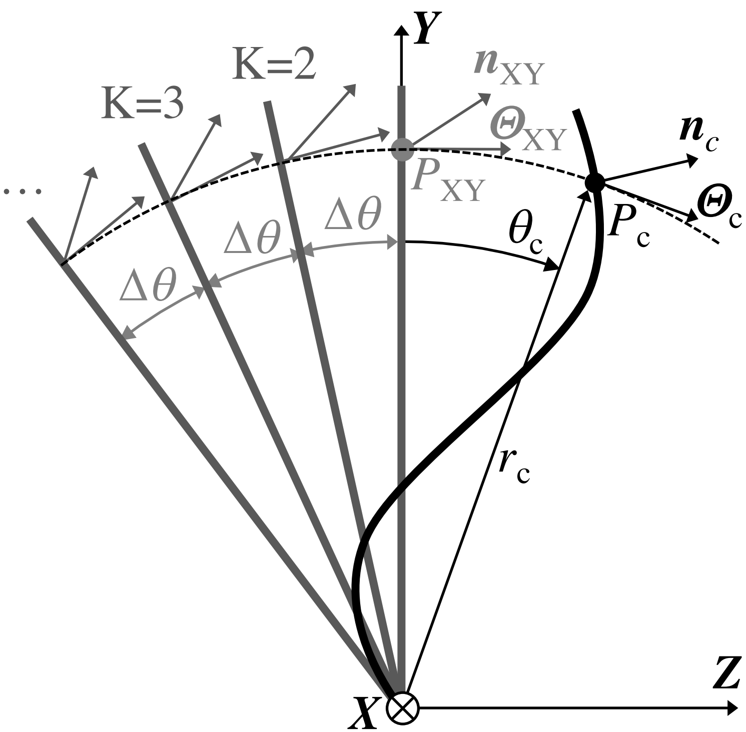

Implementation of the body force model

1. Import

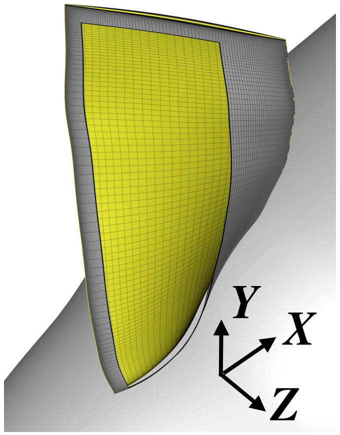

2. Extract:

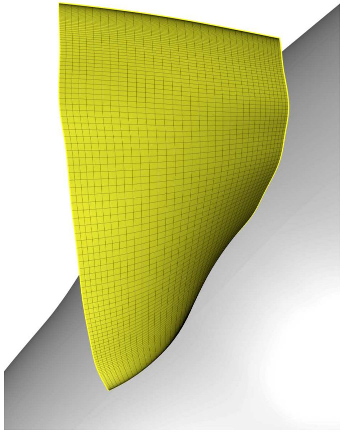

3. Flatten:

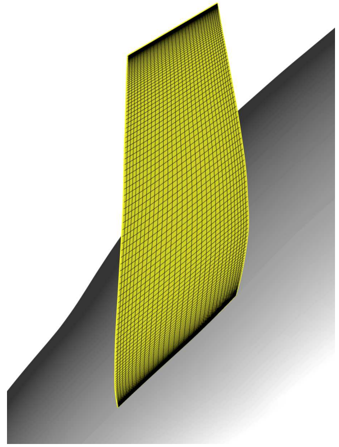

4. Extend:

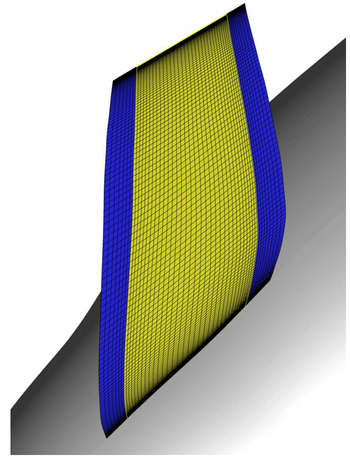

5. Revolve:

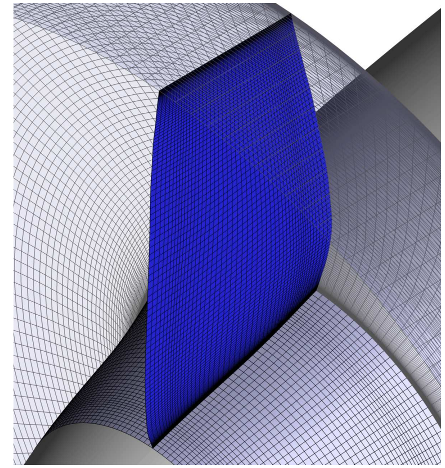

6. Rotate:

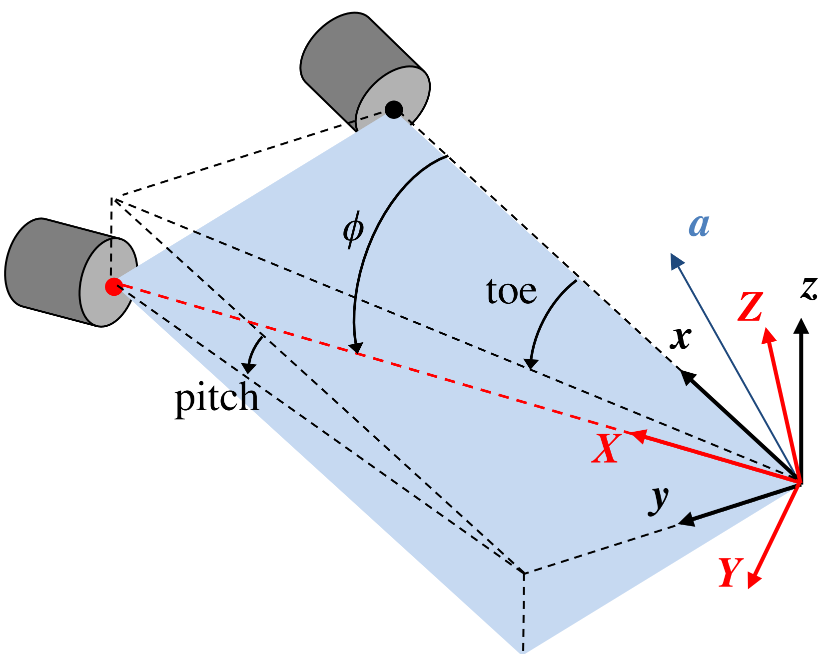

Rotate the whole grid for pitch and toe angles

Implementation of the body force model

1. Import

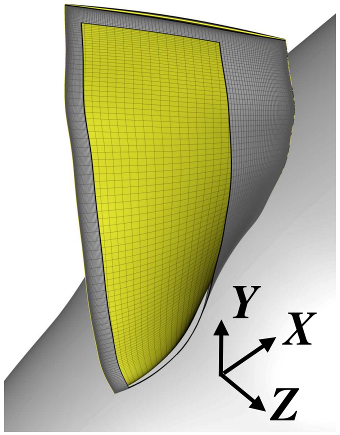

2. Extract:

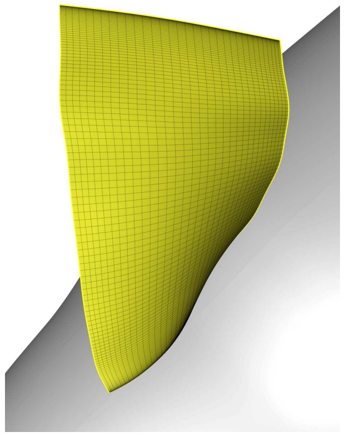

3. Flatten:

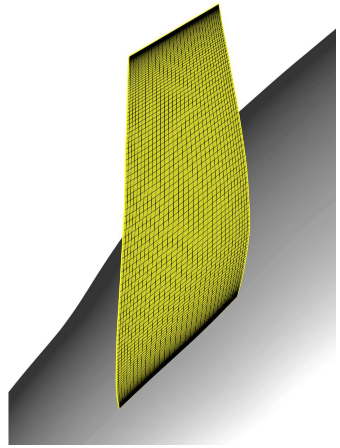

4. Extend:

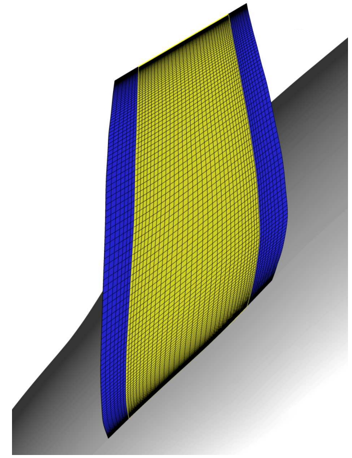

5. Revolve:

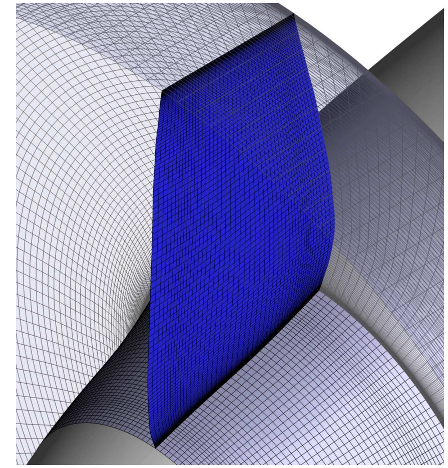

6. Rotate:

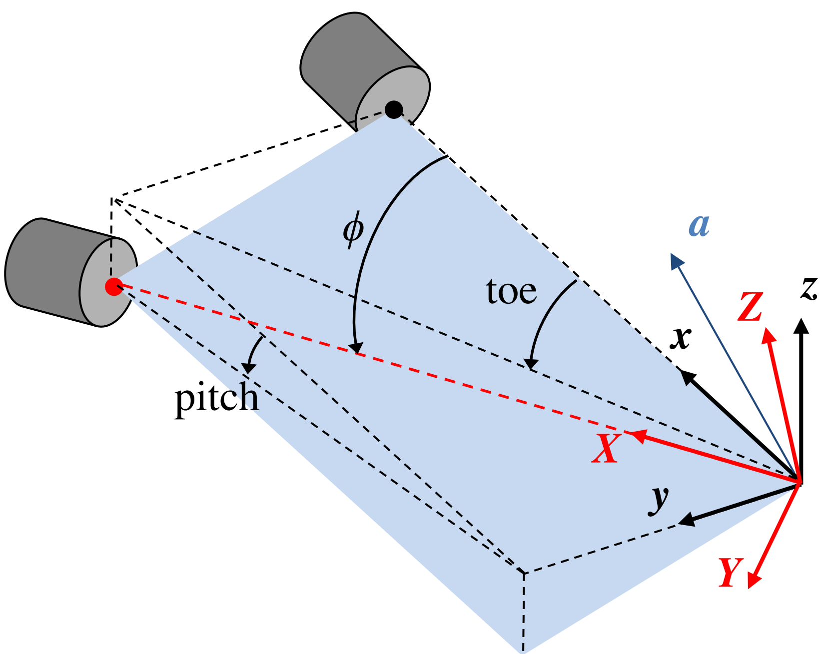

7. Save:

r

n_x

n_y

n_z

n_θ

Θ_x

Θ_y

Θ_z

Save the orientation metrics in a file

Implementation of the body force model

1. Import

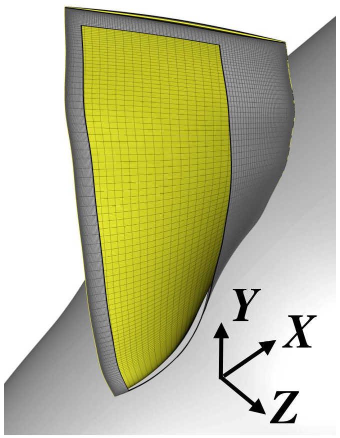

2. Extract:

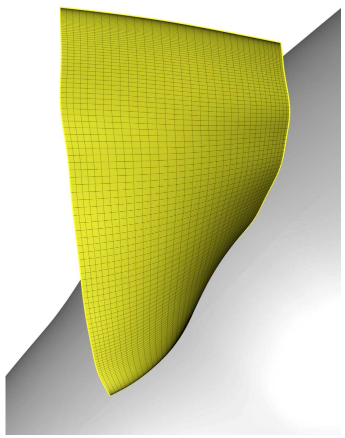

3. Flatten:

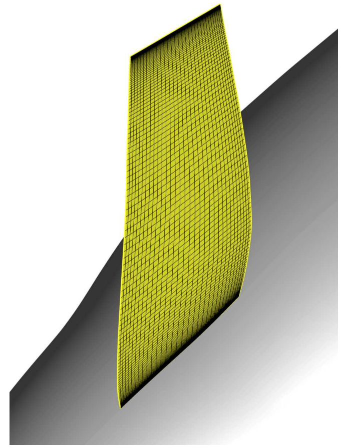

4. Extend:

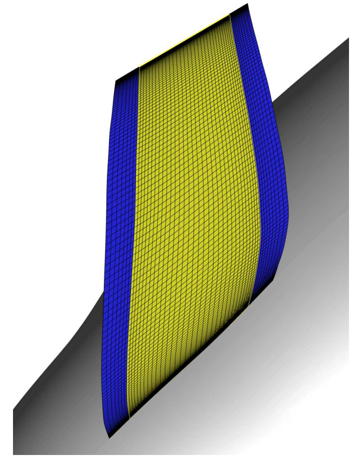

5. Revolve:

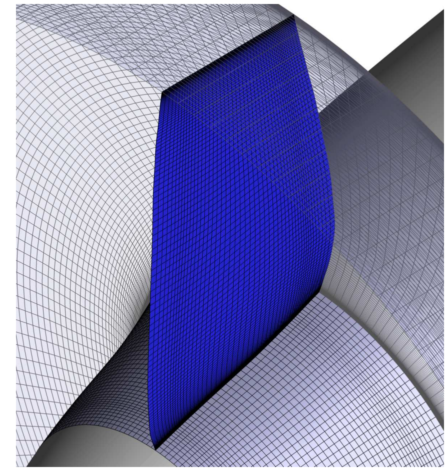

6. Rotate:

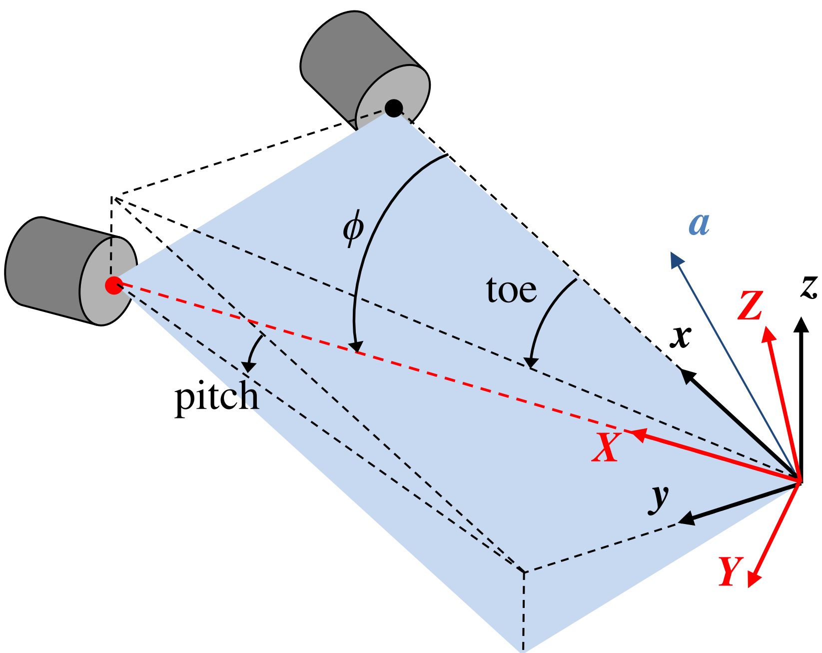

7. Save:

r

n_x

n_y

n_z

n_θ

Θ_x

Θ_y

Θ_z

8. Read in Overflow, compute the source terms at each iteration

$$f = \frac{2\pi\delta(\frac{1}{2}|\mathbf{W}|^2)}{\frac{2\pi r}{B}|n_\theta|}$$

$$\nabla \cdot (\rho \mathbf{V}) = 0$$

$$\mathbf{V} \cdot \nabla \mathbf{V} + \frac{\nabla p}{\rho} = \mathbf{f}$$

$$\mathbf{V} \cdot \nabla h_t = \mathbf{V} \cdot \mathbf{f} + \dot{e}$$

Now NS equations (not Euler equations)

Application of the Body Force Model

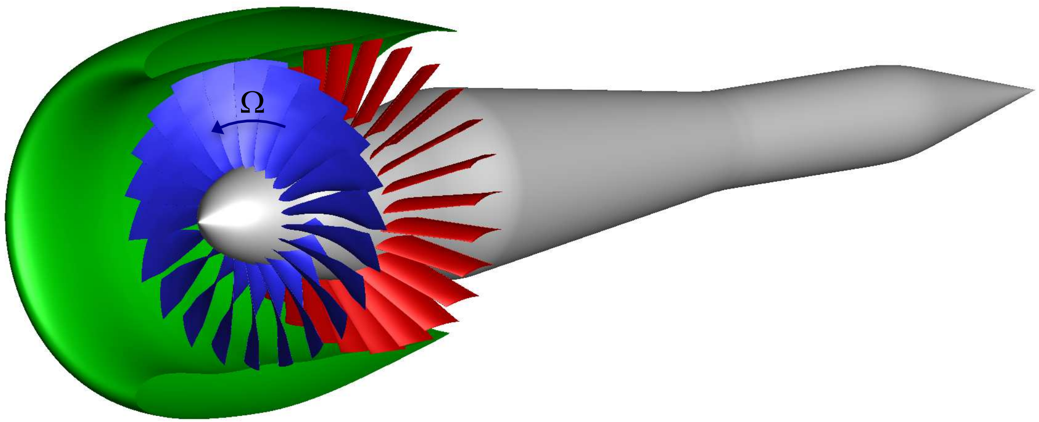

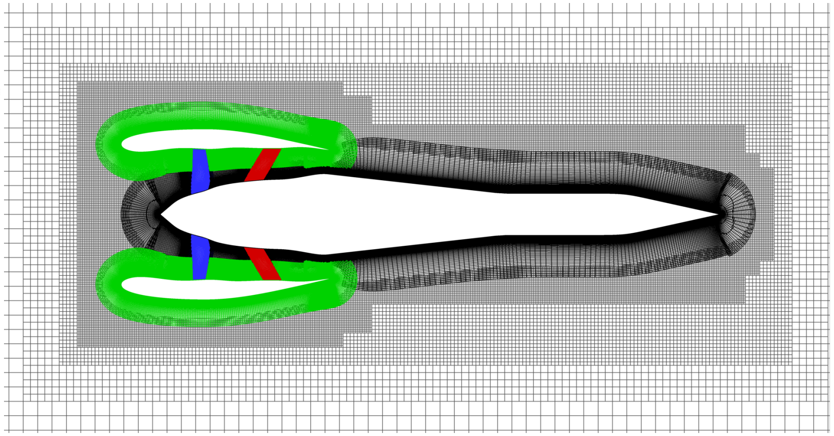

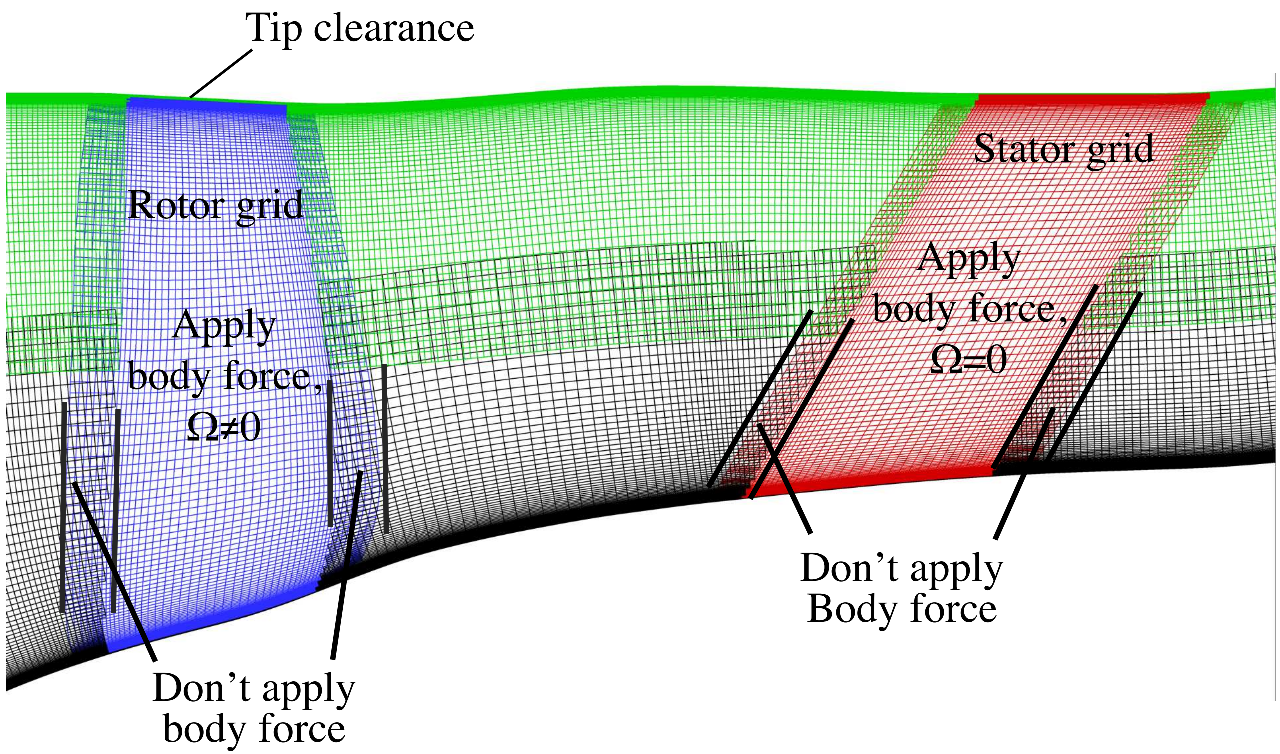

The Tools and Methods

Grid Generation: *Chimera Grid Tools (CGT)*
Steps 1 to 7 are automated by routines added to CGT codebase

Solver: *Overflow 2.2l*
An implicit RANS solver for body-fitted structured overset grid systems

Simulations here used

- Diagonalized approximate factorization scheme [Pulliam and Chaussee 1981]
- Central difference in Euler terms
- Steady-state simulations with constant CFL number
- Matrix dissipation
- Spalart Allmaras (SA) turbulence model (SA-noft2 implementation in Overflow)
- Body force method grids and metric files are automatically split
- No multigrid when the body force model is used
- Jacobians of source terms are not added to left hand side
  (Hence no low Mach preconditioning when the body force model is used)

Nichols and Buning, *Users Manual for OVERFLOW 2.2*, https://overflow.larc.nasa.gov
Chan, Gomez, Rogers and Buning, *Best Practices in Overset Grid Generation*, 2002, AIAA-2002-3191

Test Cases

A stand-alone Source Diagnostics Test (SDT) fan with R4 rotor blades

Test Cases

A stand-alone Source Diagnostics Test (SDT) fan with R4 rotor blades

A stand-alone TF8000 propulsor

Test Cases

A stand-alone Source Diagnostics Test (SDT) fan with R4 rotor blades

A stand-alone TF8000 propulsor

The D8 aircraft model in a wind tunnel

Source Diagnostics Test (SDT) fan with R4 Rotors

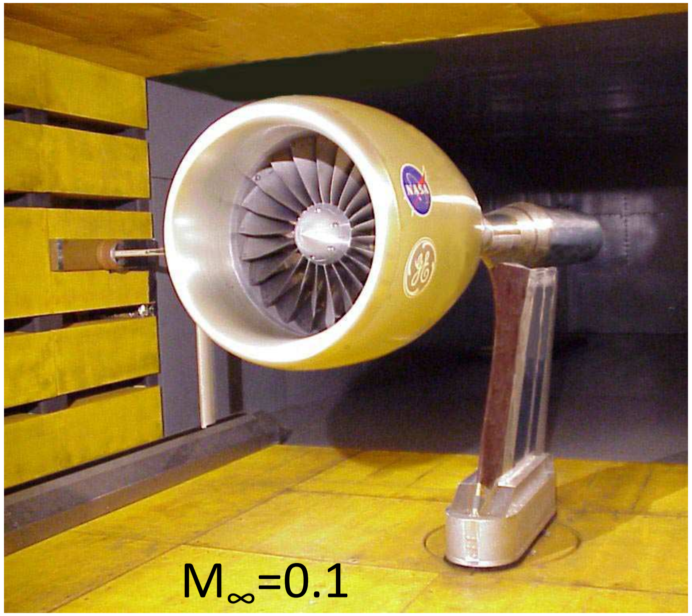

Envia, E., “Fan Noise Source Diagnostic Test Completed and Documented,”
NASA Tech. Memo. TM-2003-211990

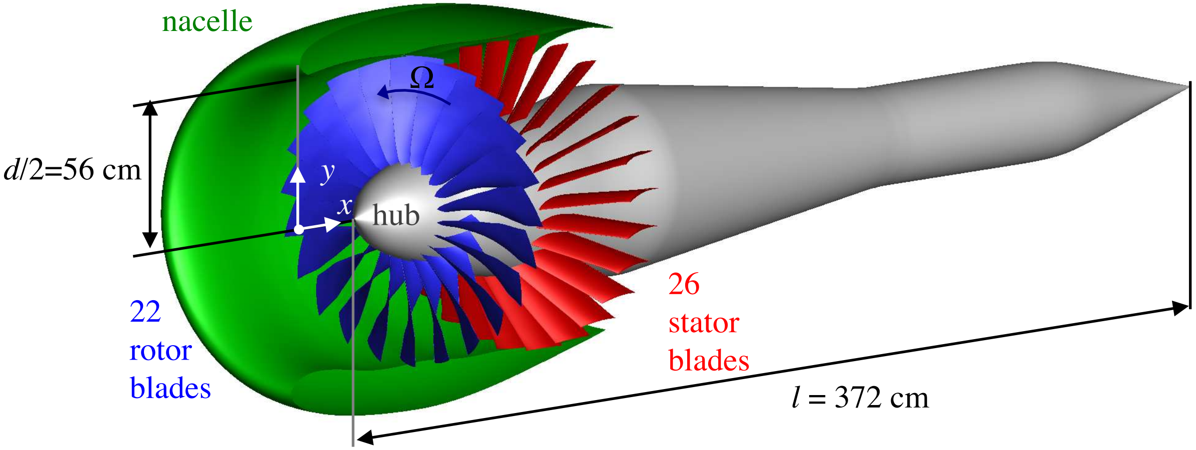

Source Diagnostics Test (SDT) fan with R4 Rotors

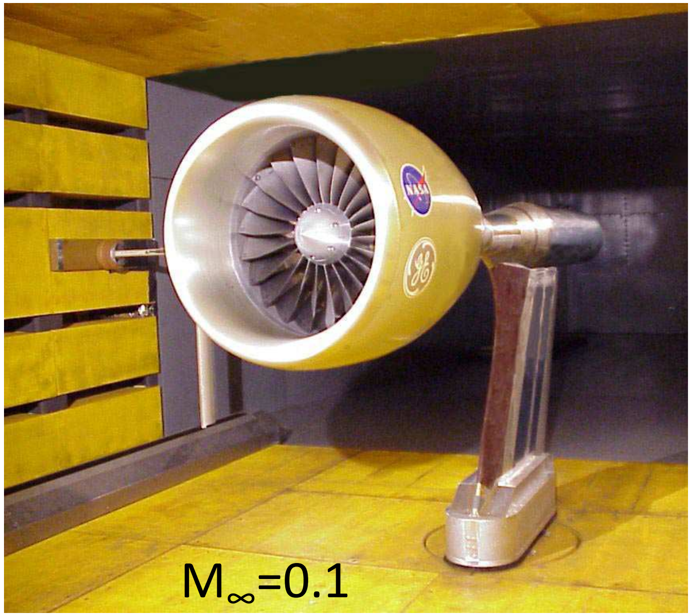

Envia, E., "Fan Noise Source Diagnostic Test Completed and Documented," NASA Tech. Memo. TM-2003-211990

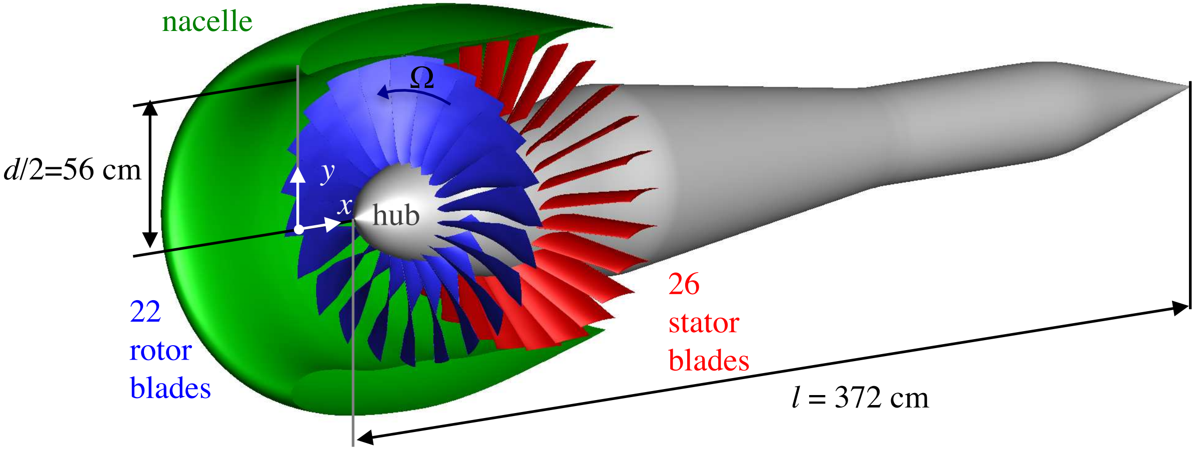

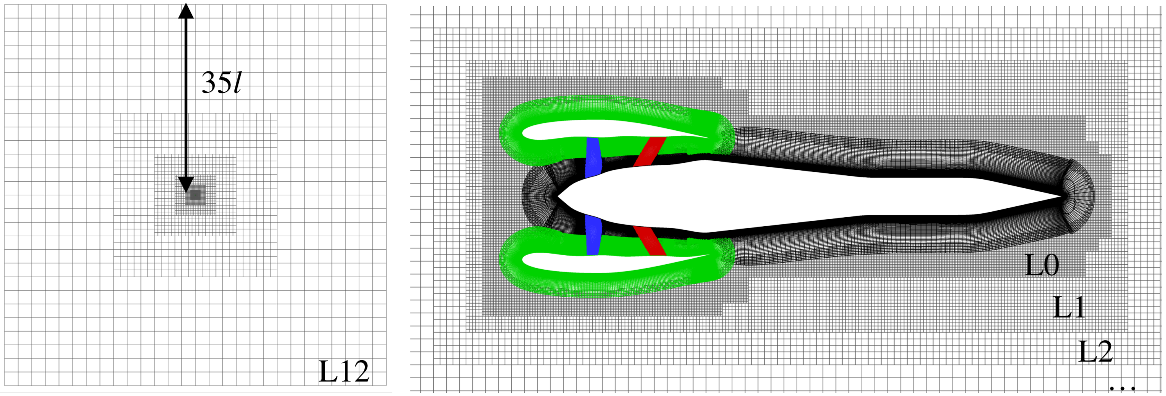

35 million vertices, $y^+ \approx 1$
4 to 8 hours on 128 Haswell cores

Full convergence with body force model
Partial convergence with pressure jump

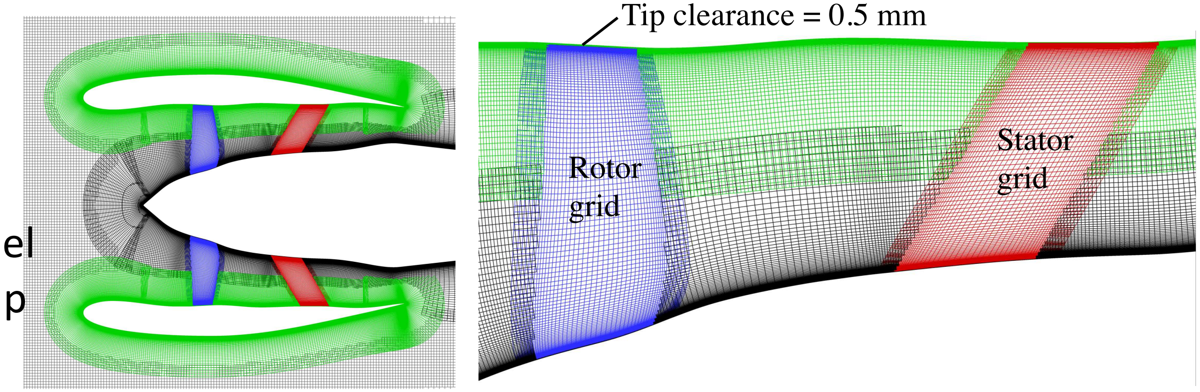

SDT fan results

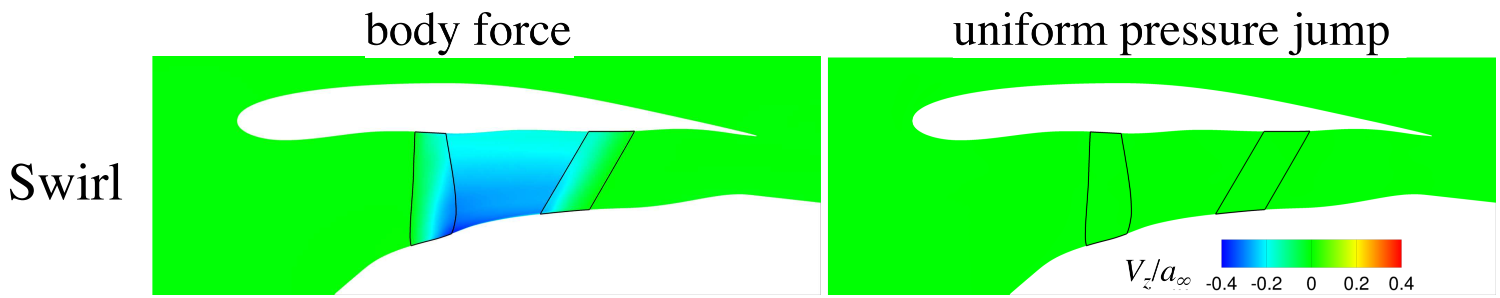

SDT fan results

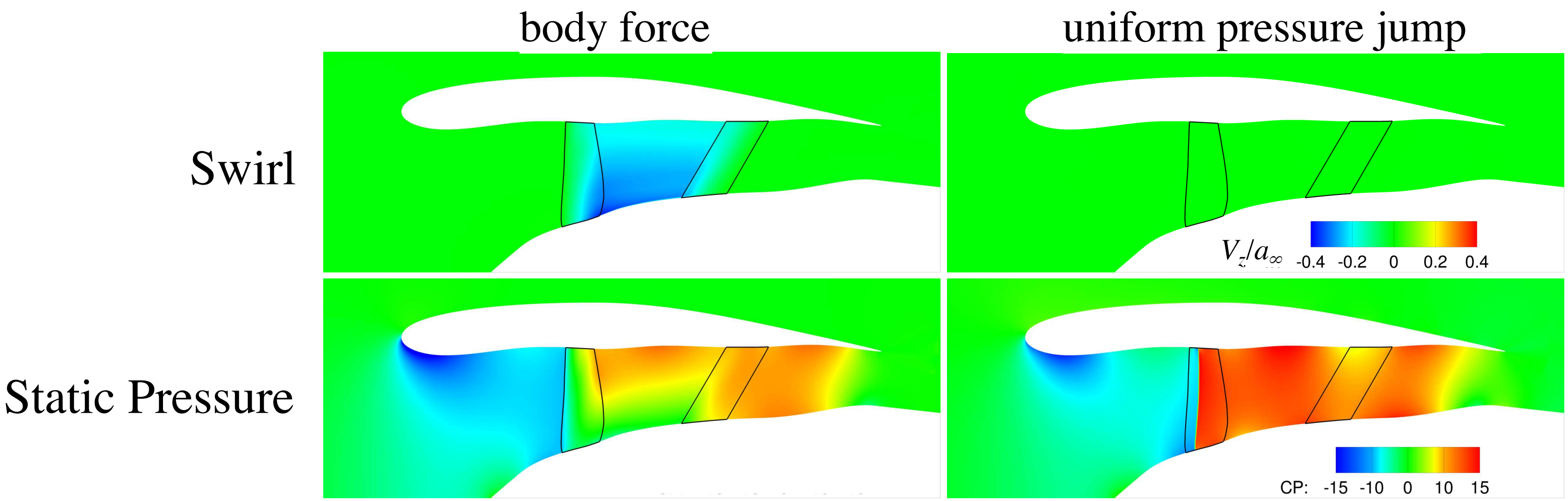

SDT fan results

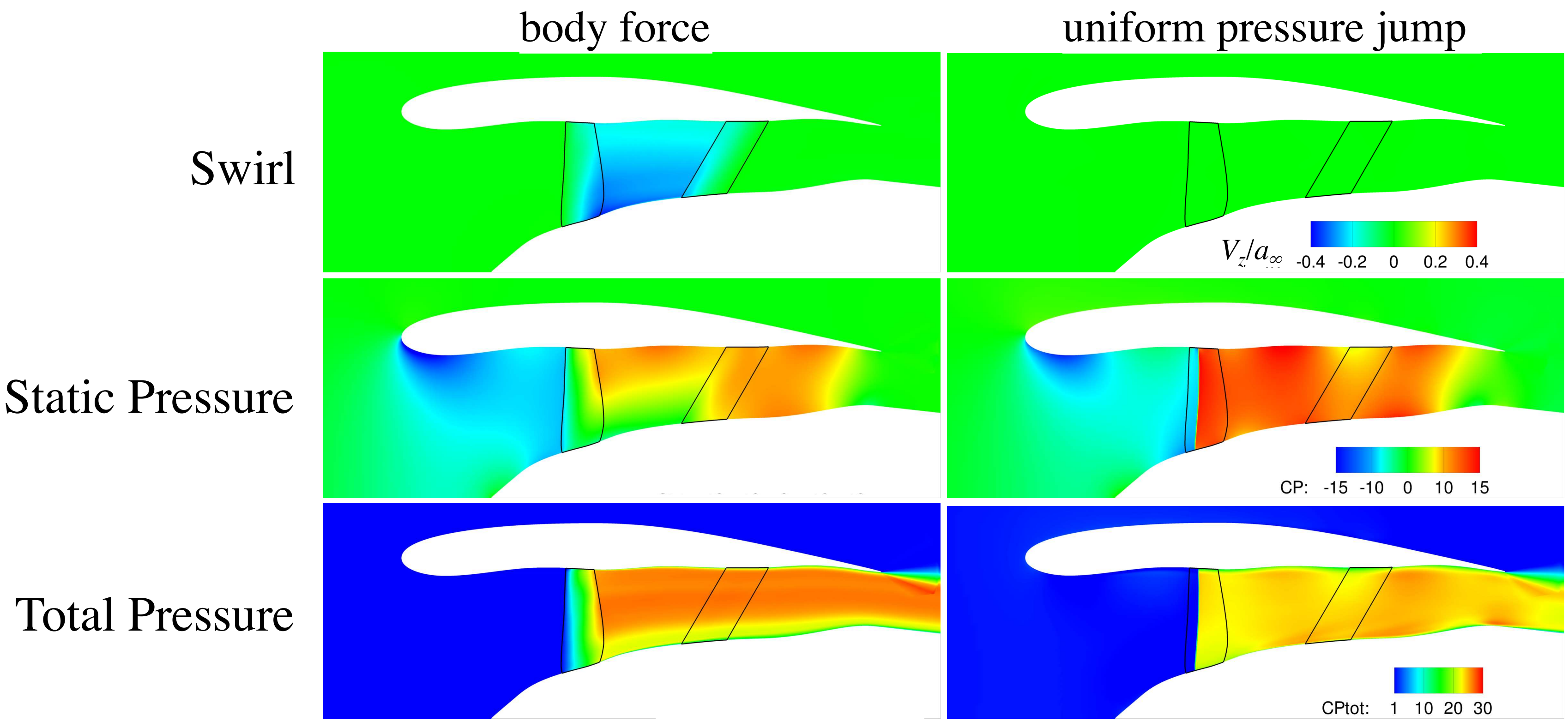

SDT fan results

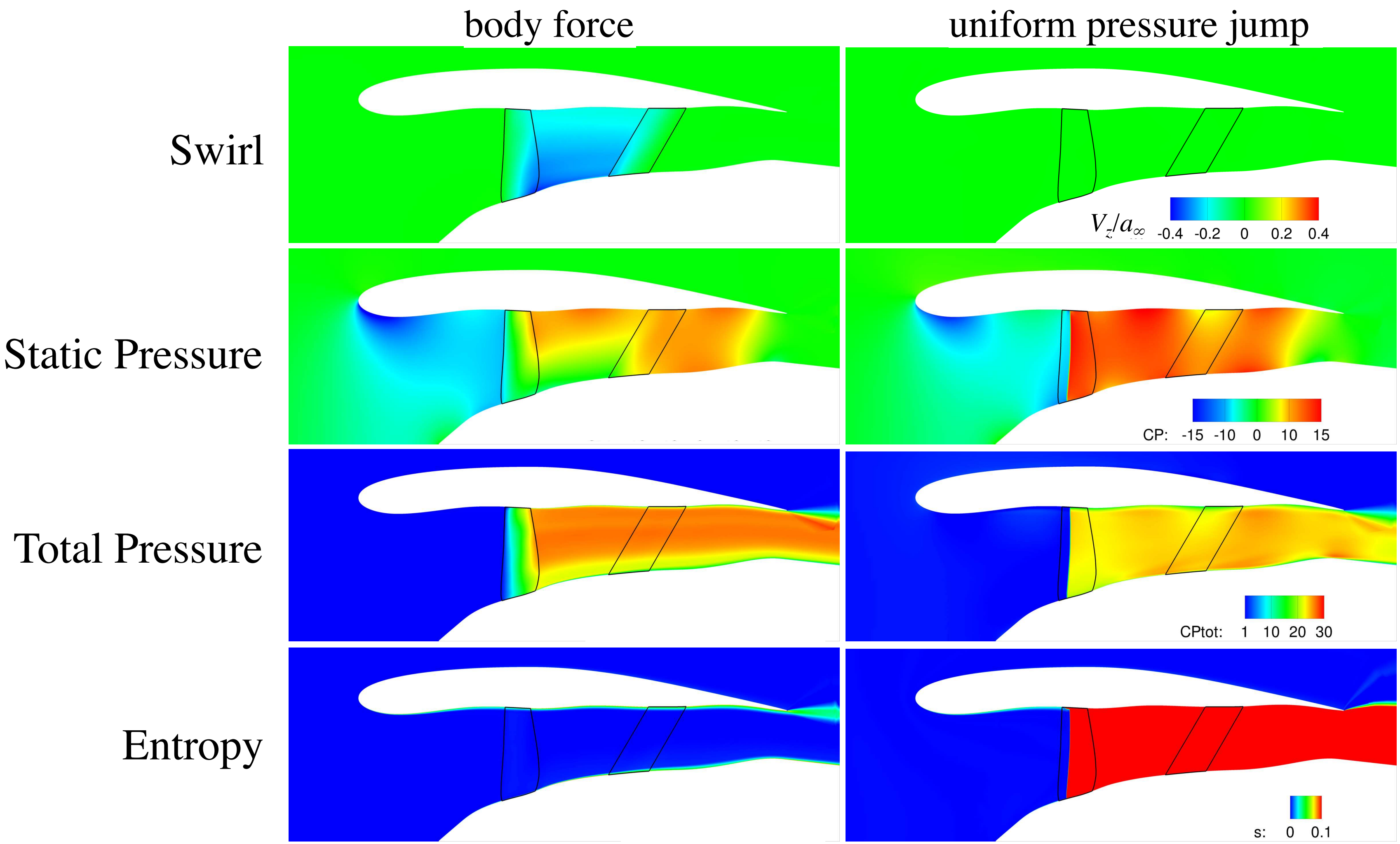

SDT fan results

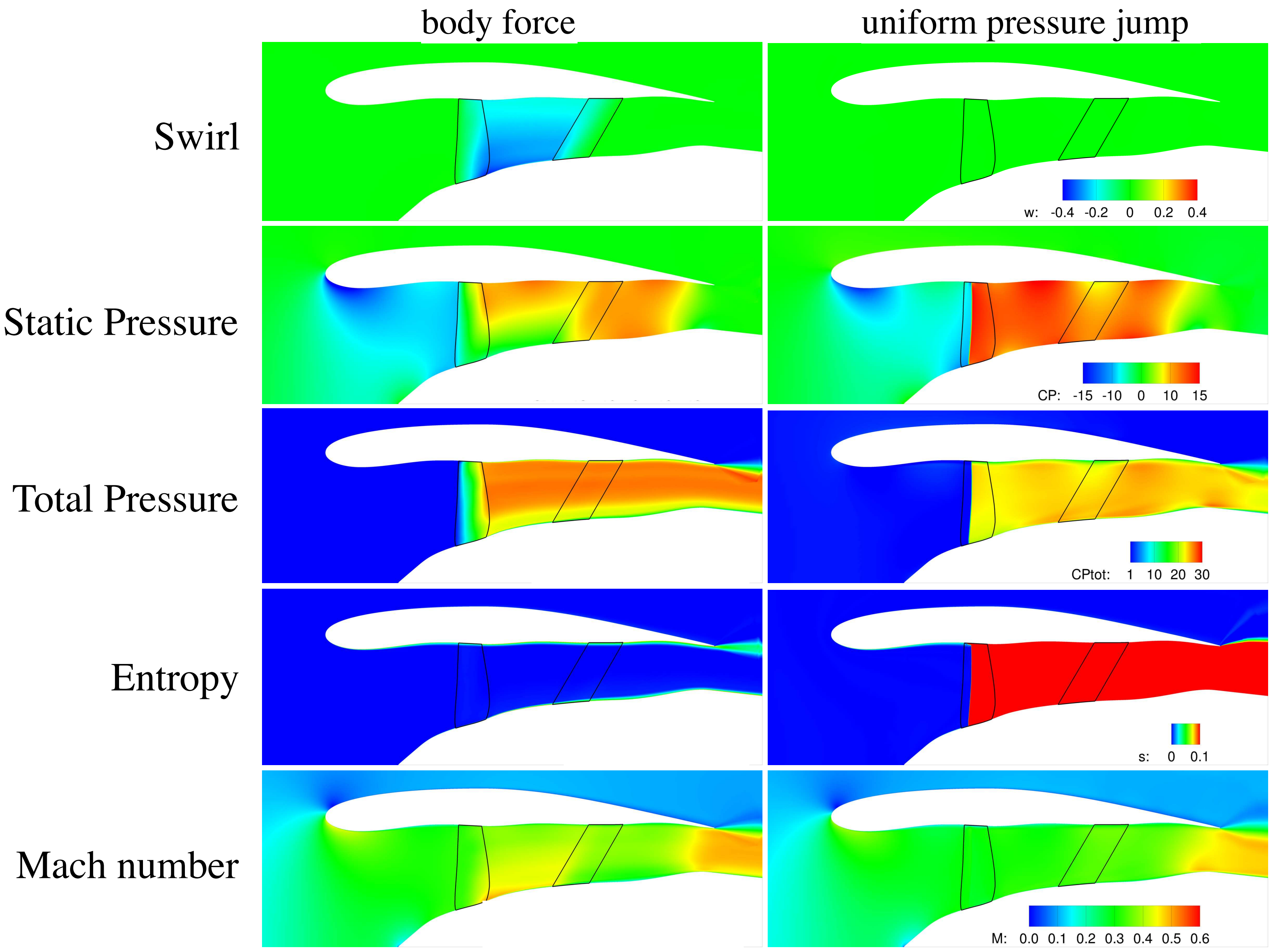

SDT fan results

body force | uniform pressure jump

Streamlines

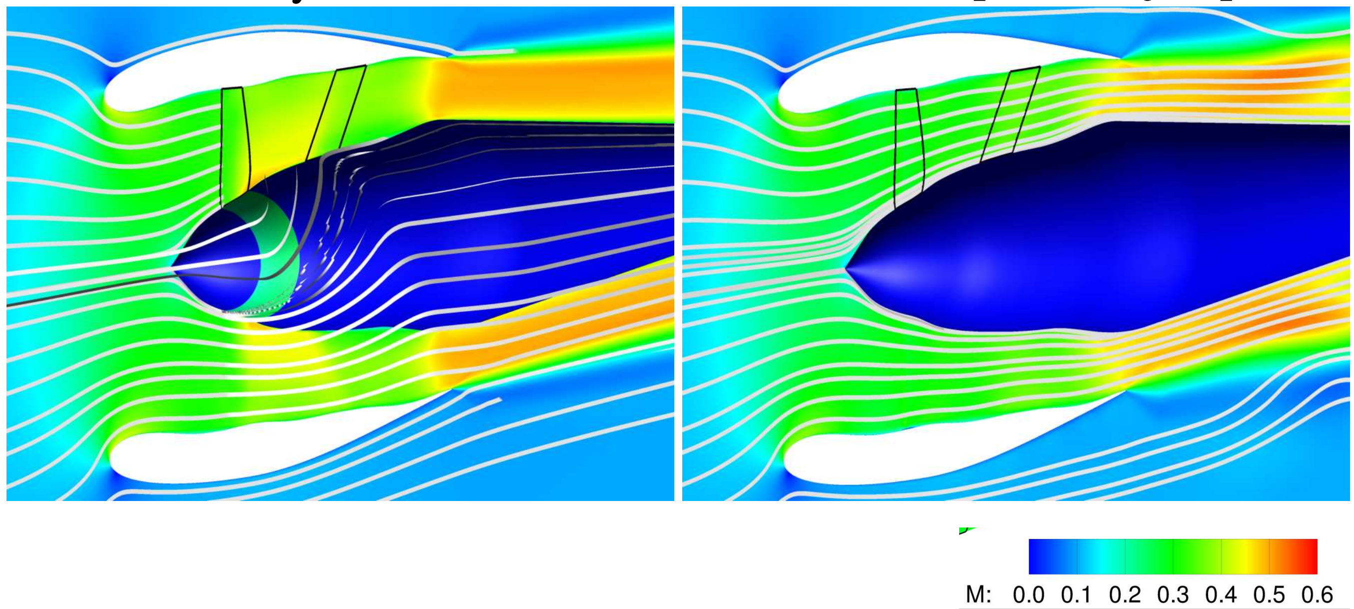

SDT fan results

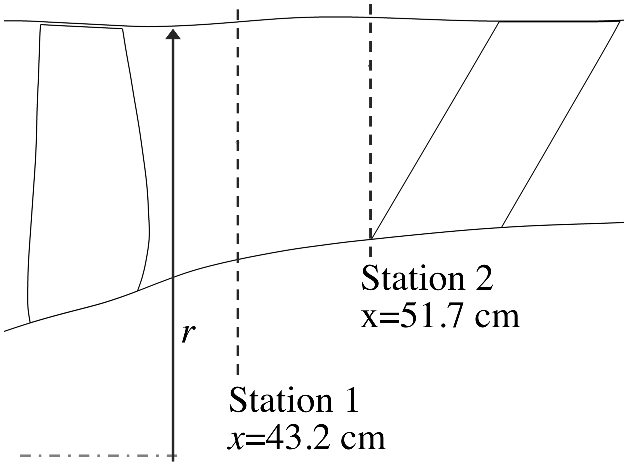

SDT fan results

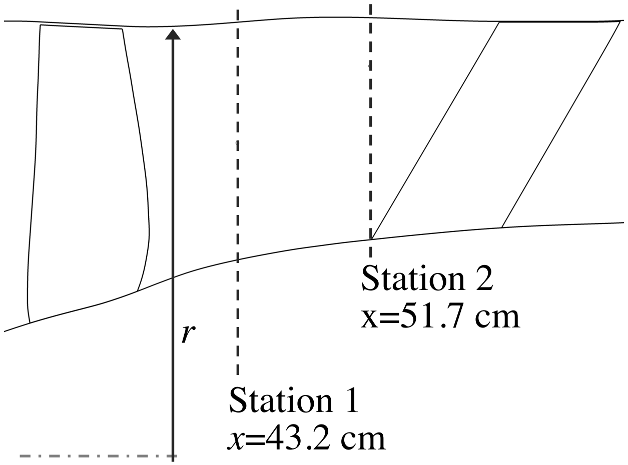

7,808 rpm 12,657 rpm

7,808 rpm	12,657 rpm		
——	——	Experiment (phase-avg.)	SDT campaign at NASA Glenn Research Center POC: Dr. Ed Envia
- - -	- - -	Experiment (mean of phase-avg.)	
——	——	Simulation (body force model)	

SDT fan results

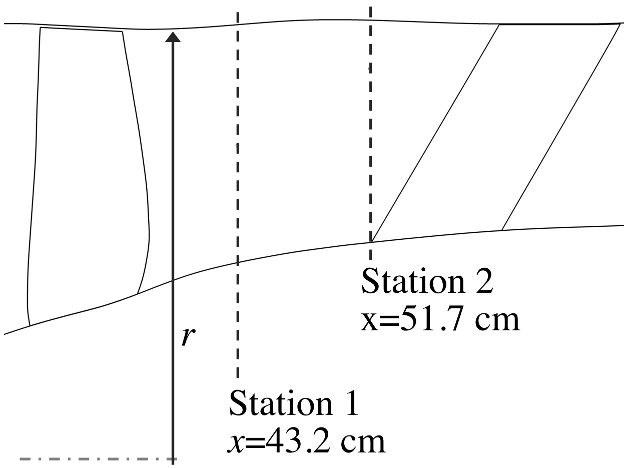

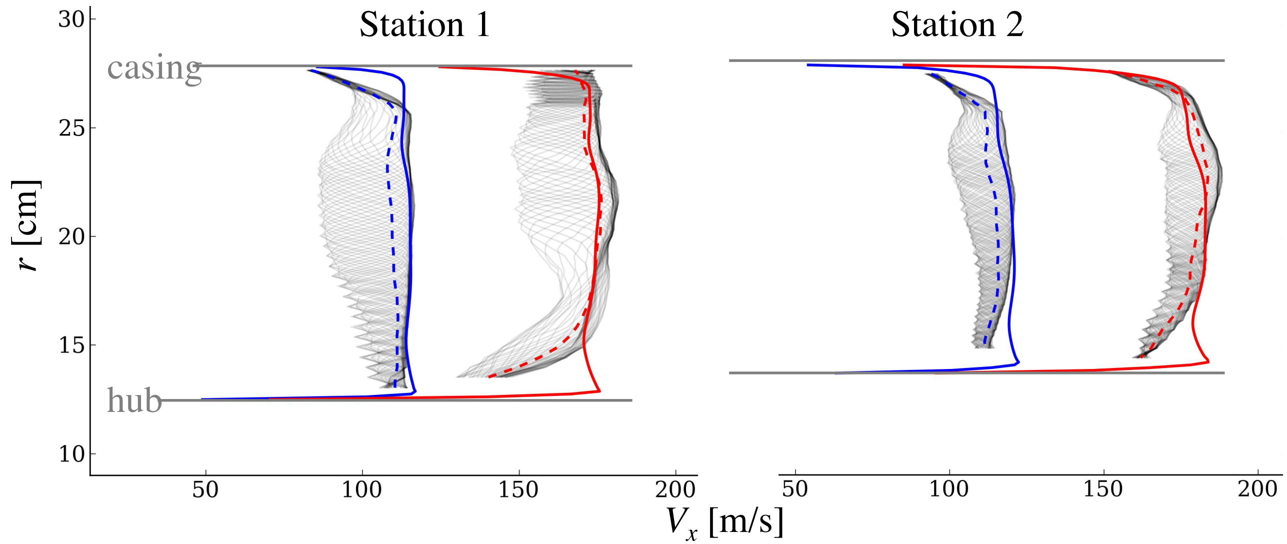

7,808 rpm 12,657 rpm

Experiment (phase-avg.)

Experiment (mean of phase-avg.)

Simulation (body force model)

SDT fan results

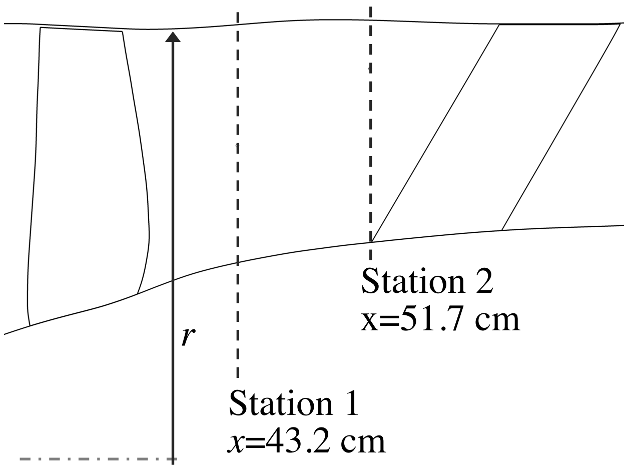

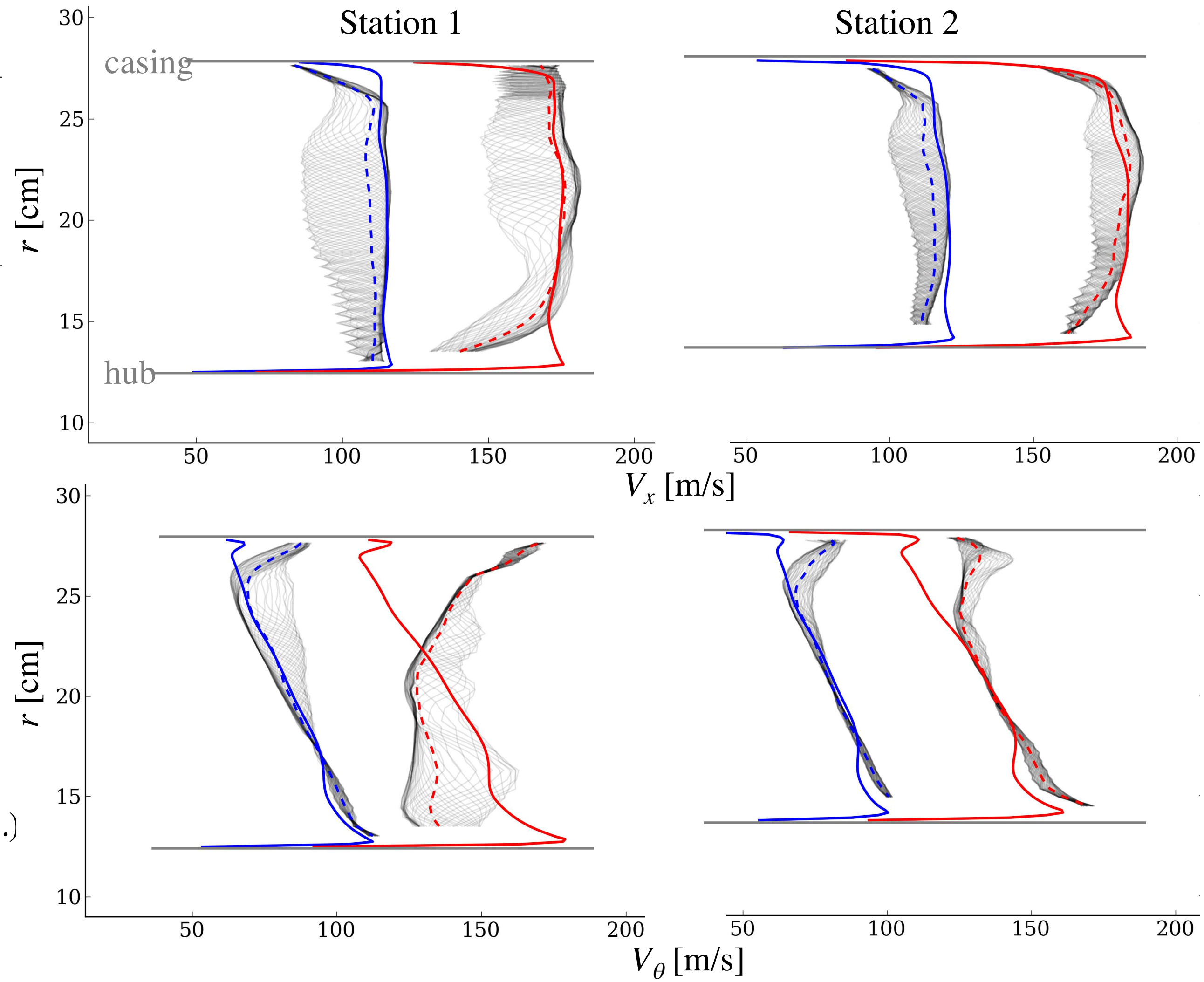

7,808 rpm 12,657 rpm

Experiment (phase-avg.)

Experiment (mean of phase-avg.)

Simulation (body force model)

SDT fan results

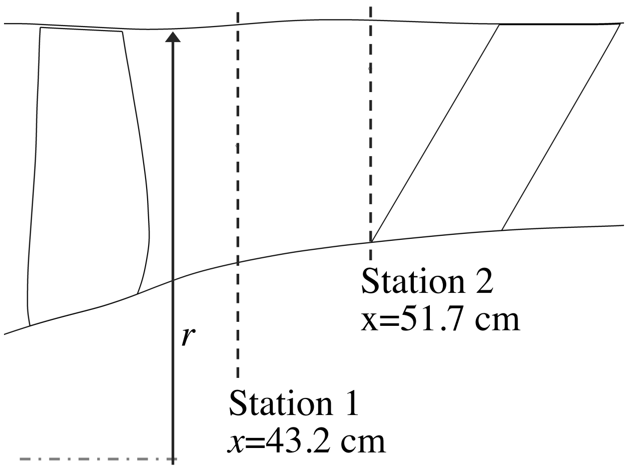

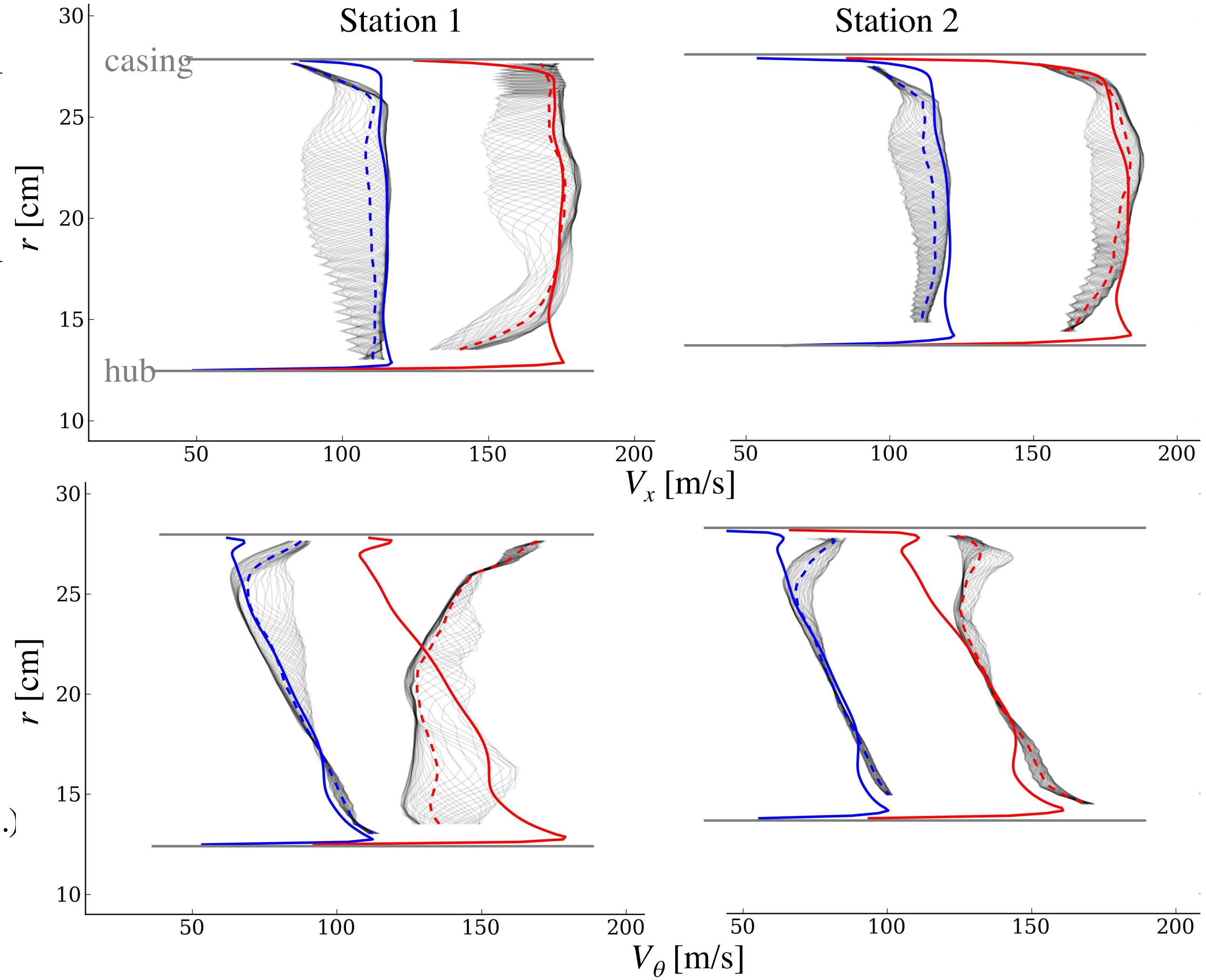

7,808 rpm 12,657 rpm

Experiment (phase-avg.)

Experiment (mean of phase-avg.)

Simulation (body force model)

at Station 1, Ω=12,657 rpm	$\bar{V}_x$ [m/s]	$\bar{V}_\theta$ [m/s]	$P_{o,1}$ / $P_{o,\infty}$
Experiment	171	138	1.509
Body Force Model	172	133	1.491

Hughes et al., 2005

The D8 aircraft in wind tunnel

Tests 14x22ft Wind Tunnel at NASA Langley Research Center

Uranga *et al.*, *Preliminary Experimental Assessment of the Boundary Layer Ingestion Benefit for the D8 Aircraft*, AIAA-2014-0906

CFD (Computational Fluid Dynamics) simulations of the model in the wind tunnel

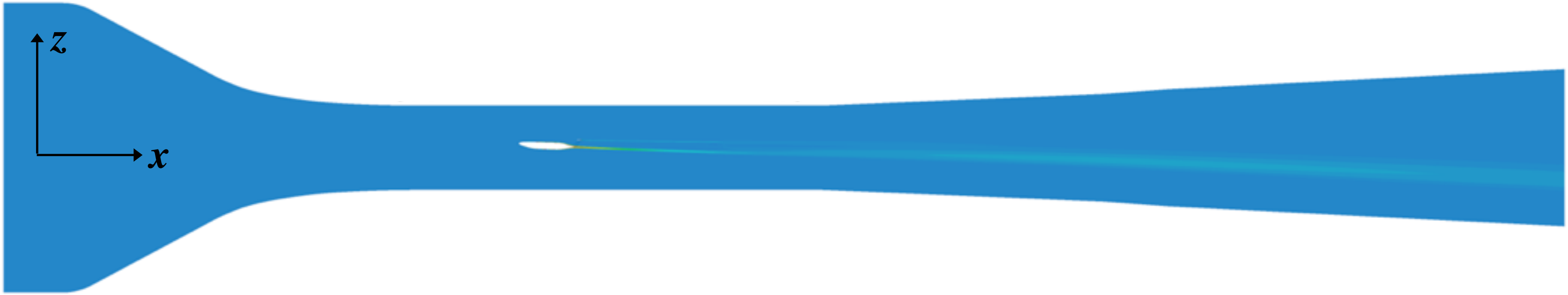

Pandya, *External Aerodynamics Simulations for the MIT D8 "Double-Bubble" Aircraft Design*, 2012, ICCFD7-4304

TF8000 propulsor on D8

TF8000 propulsor

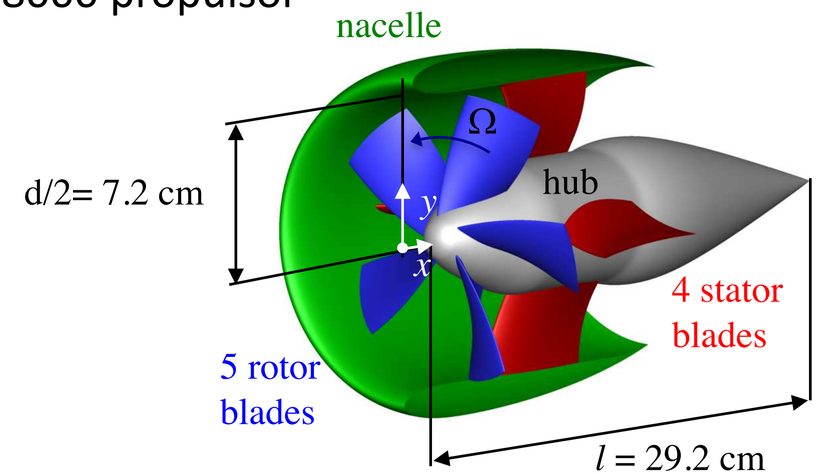

D8 aircraft in wind tunnel

200 million vertices, $y^+ \approx 1$
30 to 40 hours on 800 Haswell cores

TF8000 propulsor on D8 -- Results

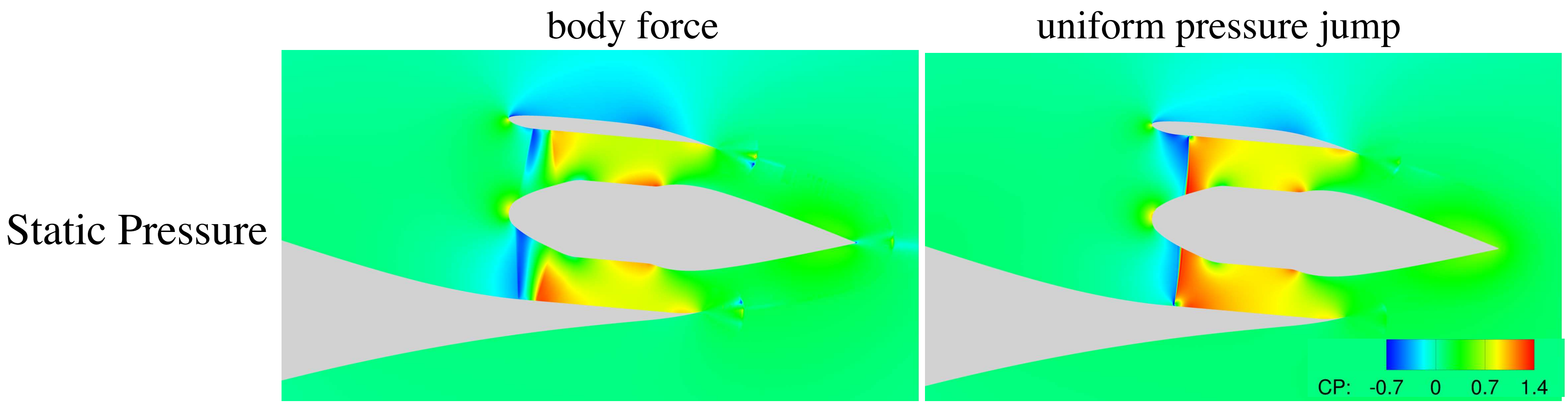

TF8000 propulsor on D8 -- Results

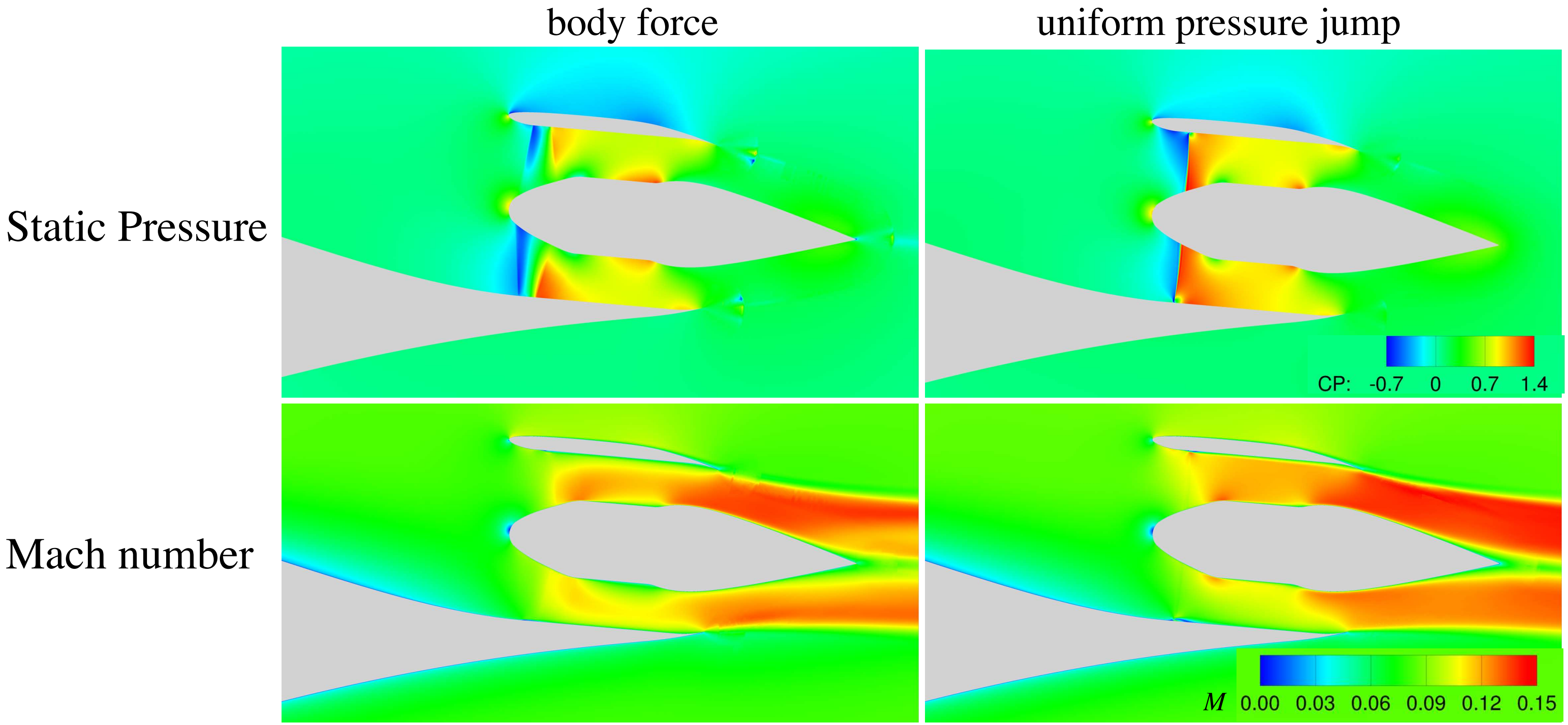

TF8000 propulsor on D8 -- Results

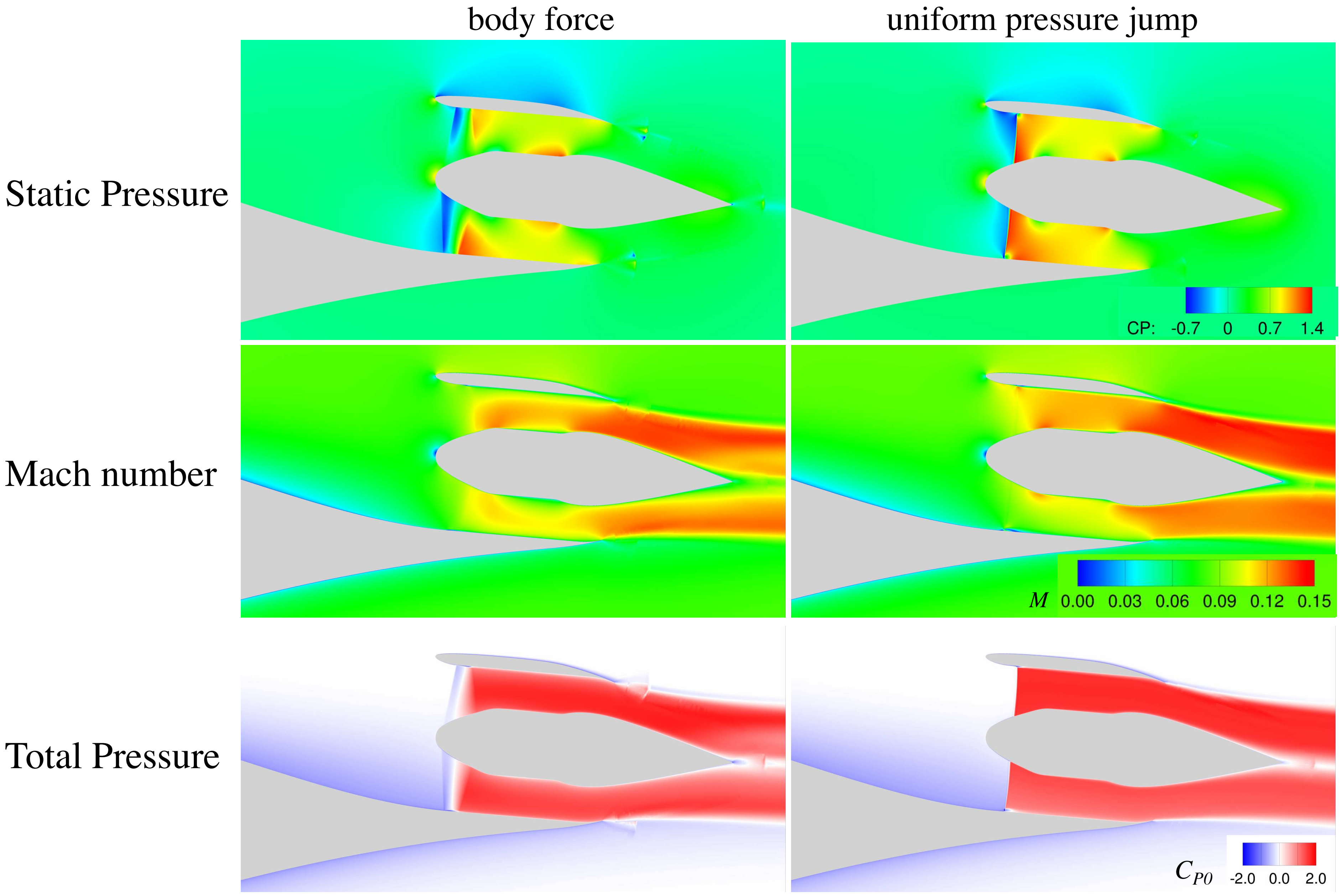

TF8000 propulsor on D8 -- Results

$$\Delta C_{P0} = C_{P0,\text{body force}} - C_{P0,\text{pressure jump}}$$

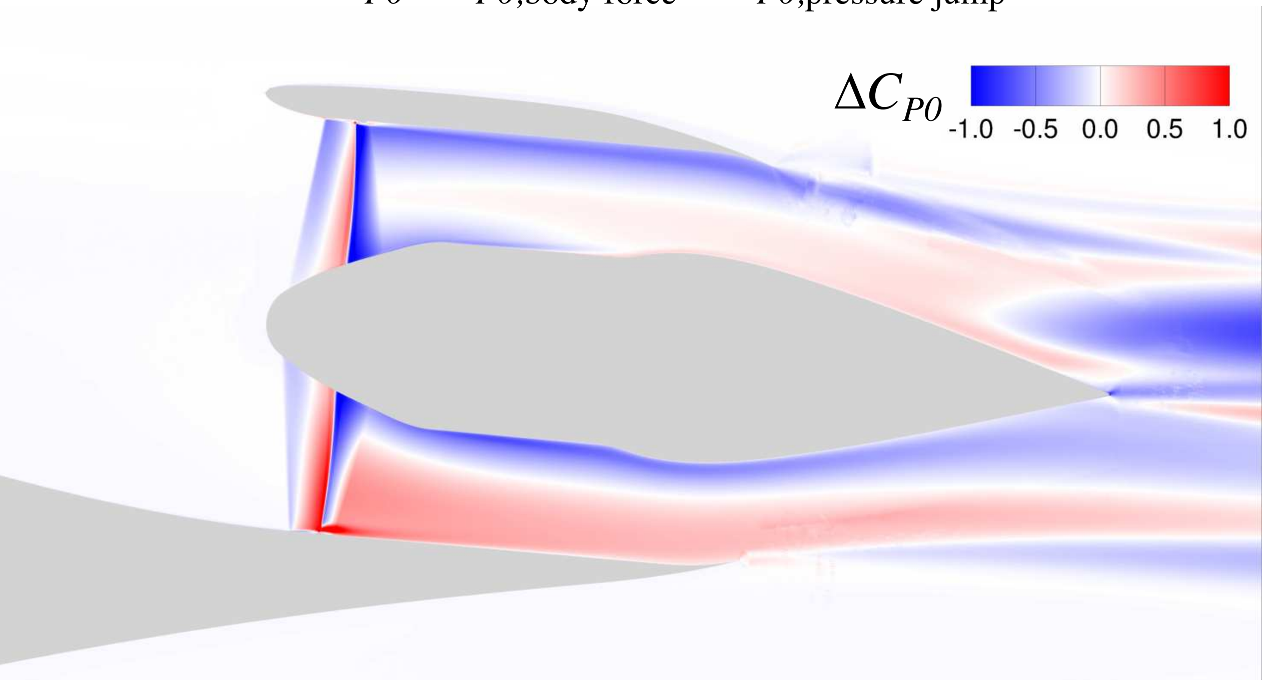

TF8000 propulsor on D8 -- Results

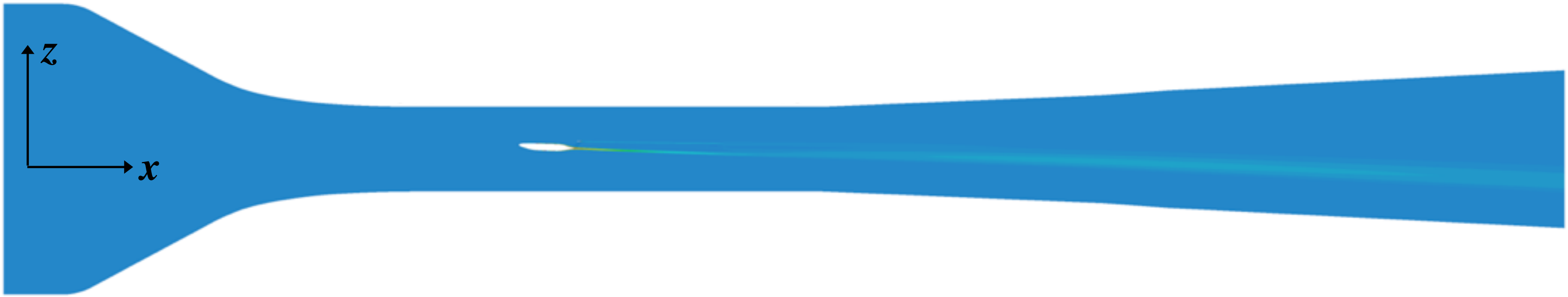

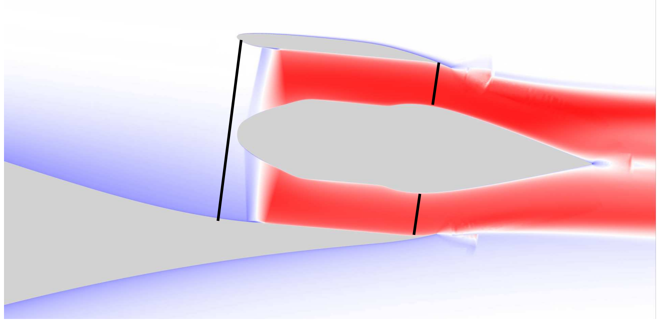

$$C_{\text{PK}} = \frac{\int_{fan} (p_{t,\infty} - p_t)(\mathbf{V} \cdot \mathbf{n}) \, dA}{q_\infty V_\infty S_{ref}}$$

TF8000 propulsor on D8 -- Results

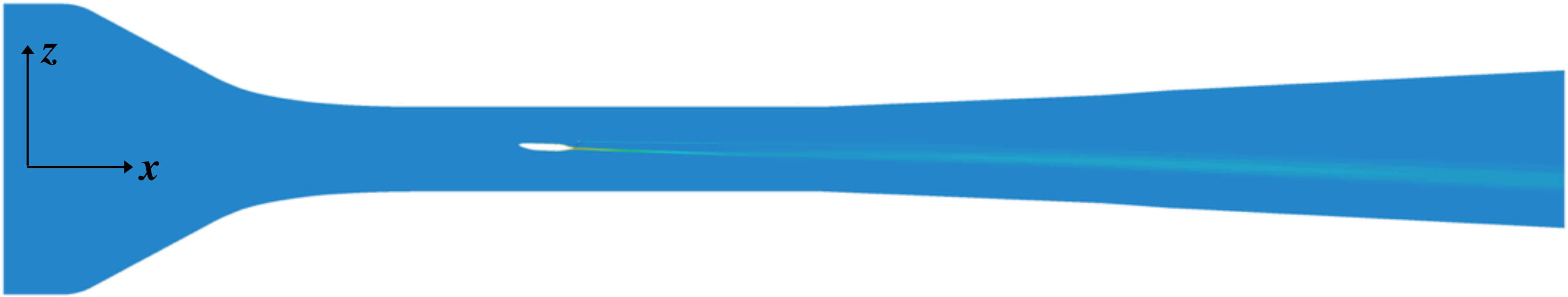

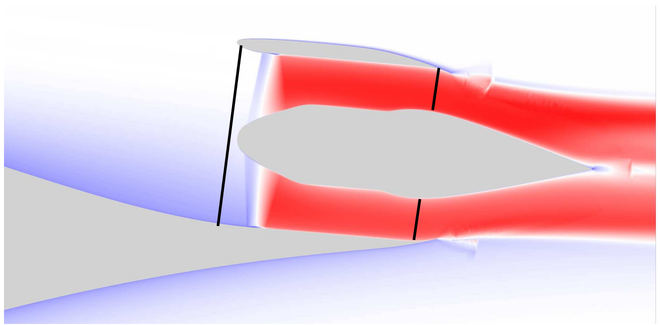

$$C_{\mathrm{PK}} = \frac{\int_{fan} (p_{t,\infty} - p_t)(\mathbf{V} \cdot \mathbf{n}) \, dA}{q_\infty V_\infty S_{ref}}$$

Method	C_x	C_z	C_{PK}	$C_{\dot{m}}$
Experiment (11,100 rpm)	0.0000 ± 0.0006	0.644 ± 0.001	0.045 ± 0.001	0.0267 ± 0.0006
Uniform Pressure Jump	0.0002	0.651	0.045	0.0282

Experimental data inferred from Uranga et al., 2014

TF8000 propulsor on D8 -- Results

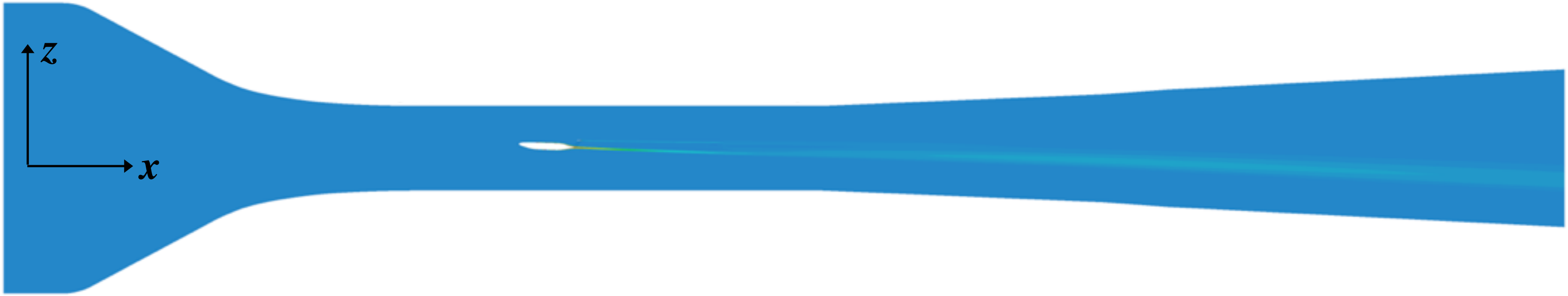

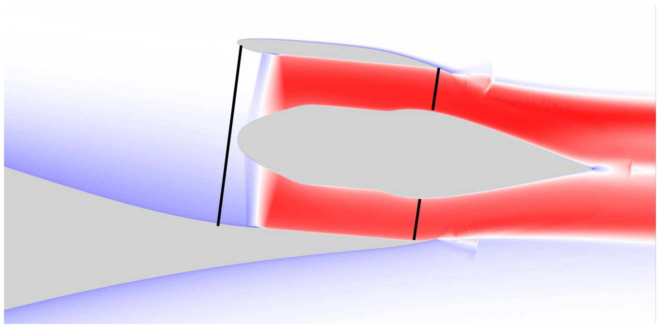

$$C_{\text{PK}} = \frac{\int_{fan} (p_{t,\infty} - p_t)(\mathbf{V} \cdot \mathbf{n})\, dA}{q_\infty V_\infty S_{ref}}$$

Method	C_x	C_z	C_{PK}	$C_{\dot{m}}$
Experiment (11,100 rpm)	0.0000 ± 0.0006	0.644 ± 0.001	0.045 ± 0.001	0.0267 ± 0.0006
Uniform Pressure Jump	0.0002	0.651	0.045	0.0282
Body Force, 11,100 rpm	0.0028	0.672	0.039	0.0275

Experimental data inferred from Uranga et al., 2014

TF8000 propulsor on D8 -- Results

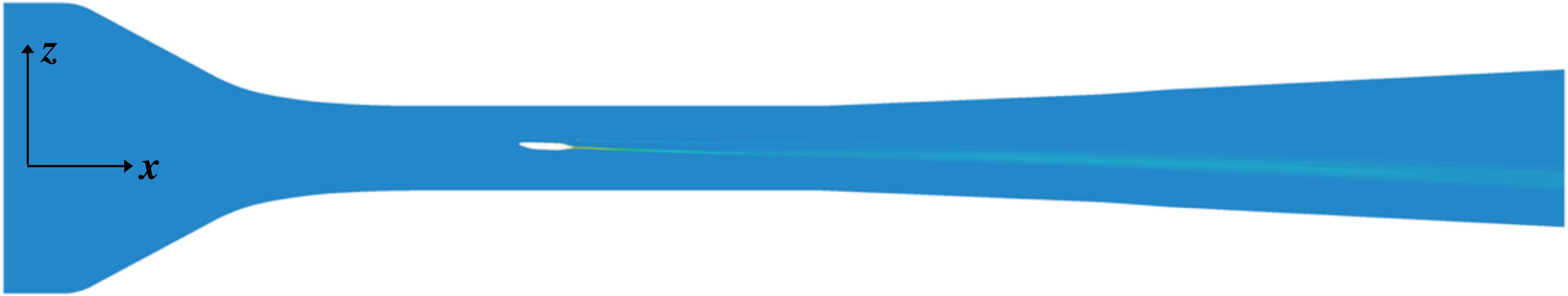

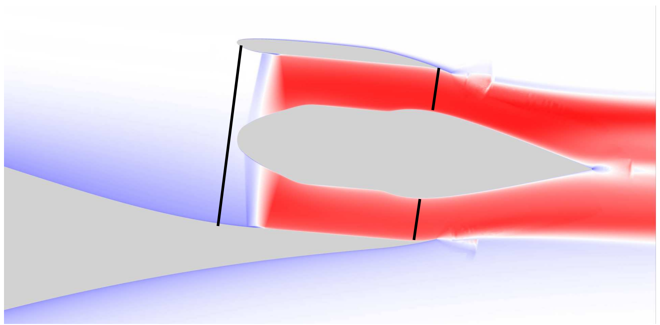

$$C_{\mathrm{PK}} = \frac{\int_{fan} (p_{t,\infty} - p_t)(\mathbf{V} \cdot \mathbf{n})\, dA}{q_\infty V_\infty S_{ref}}$$

Method	C_x	C_z	C_{PK}	$C_{\dot{m}}$
Experiment (11,100 rpm)	0.0000 ± 0.0006	0.644 ± 0.001	0.045 ± 0.001	0.0267 ± 0.0006
Uniform Pressure Jump	0.0002	0.651	0.045	0.0282
Body Force, 11,100 rpm	0.0028	0.672	0.039	0.0275
Body Force, 11,450 rpm	0.0005	0.678	0.043	0.0281

Experimental data inferred from Uranga et al., 2014

TF8000 propulsor on D8 -- Results

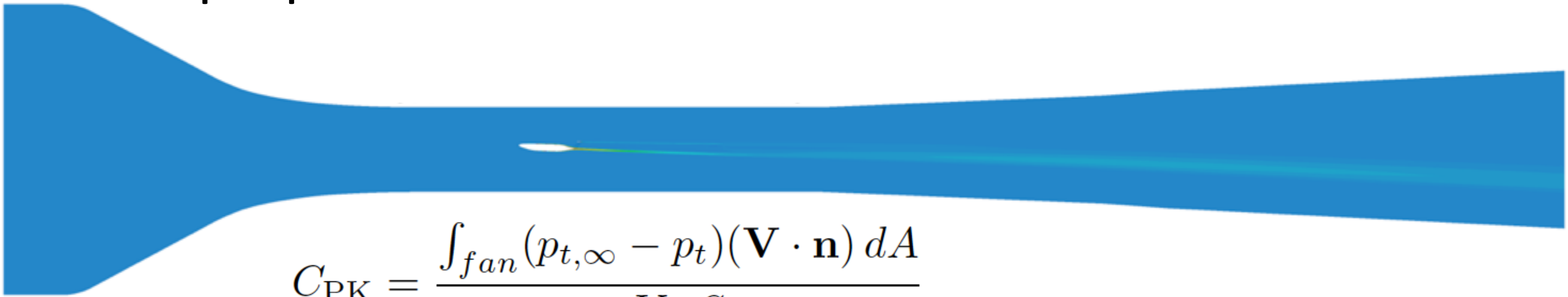

$$C_{\mathrm{PK}} = \frac{\int_{fan} (p_{t,\infty} - p_t)(\mathbf{V} \cdot \mathbf{n})\, dA}{q_\infty V_\infty S_{ref}}$$

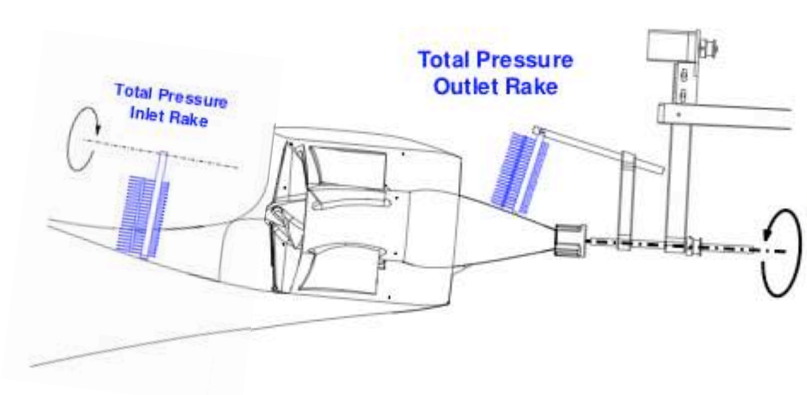

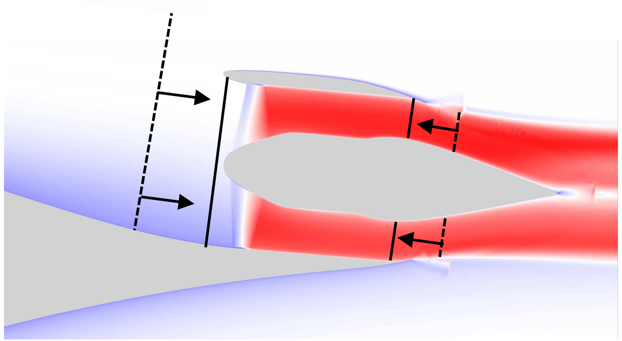

Experimental data inferred from Uranga et al., 2014

TF8000 propulsor on D8 -- Results

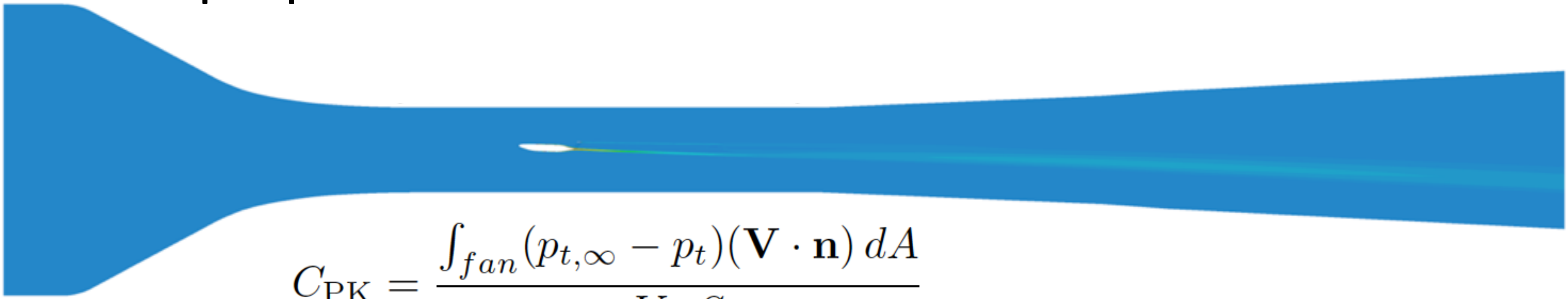

$$C_{PK} = \frac{\int_{fan}(p_{t,\infty} - p_t)(\mathbf{V} \cdot \mathbf{n})\, dA}{q_\infty V_\infty S_{ref}}$$

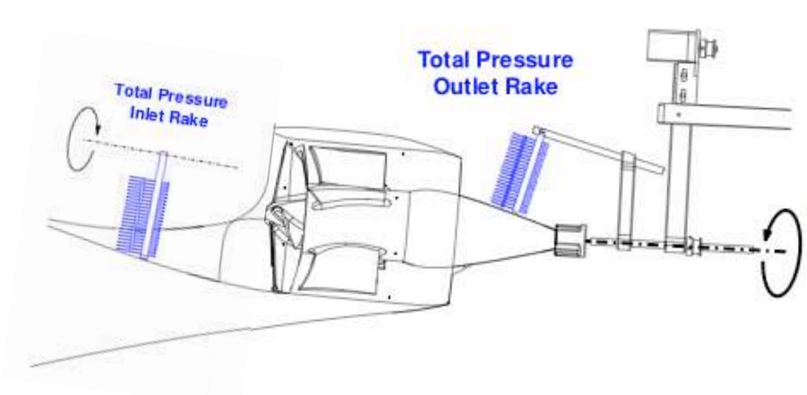

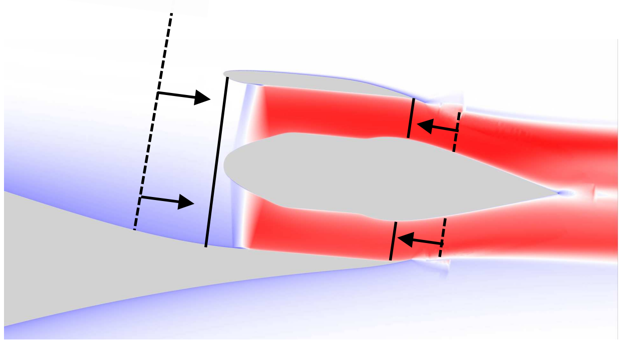

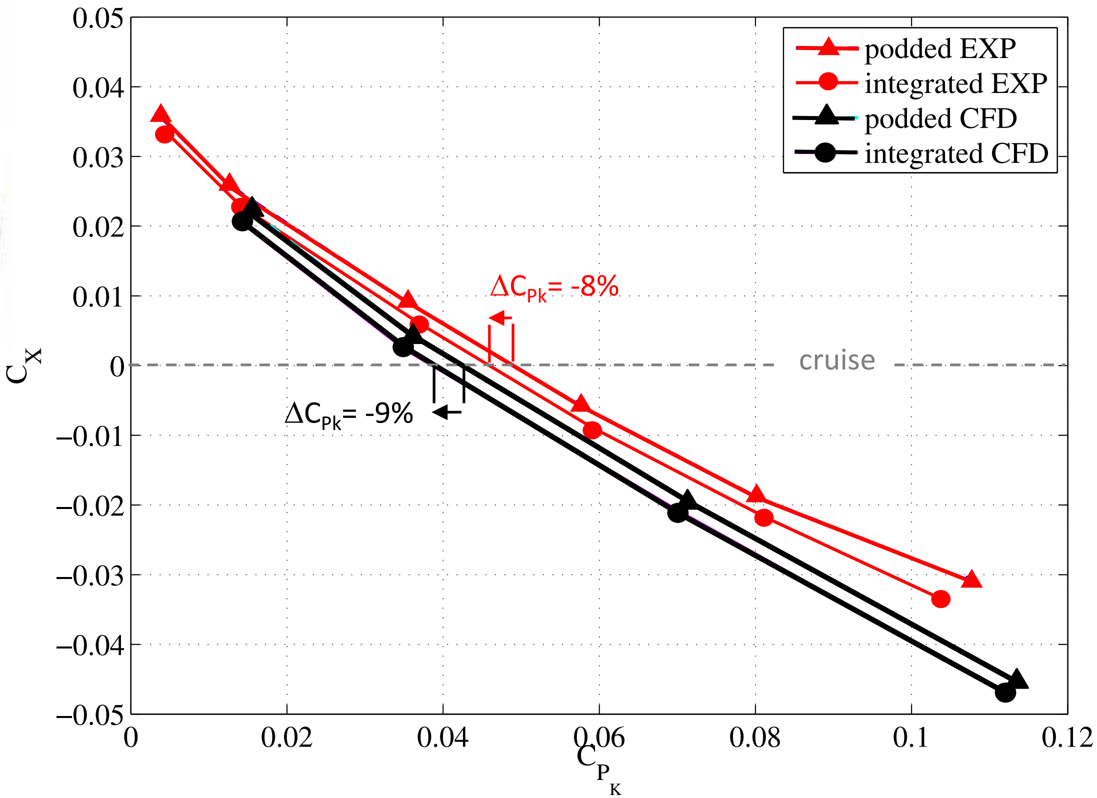

Experimental data inferred from Uranga et al., 2014

TF8000 propulsor on D8 – Swirl Effects

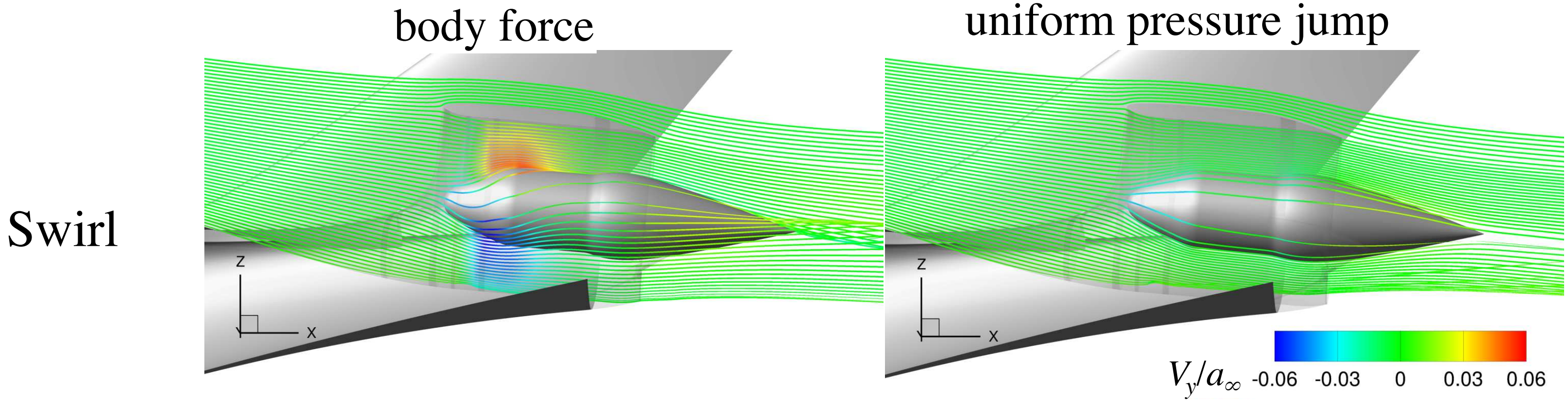

TF8000 propulsor on D8 -- Results

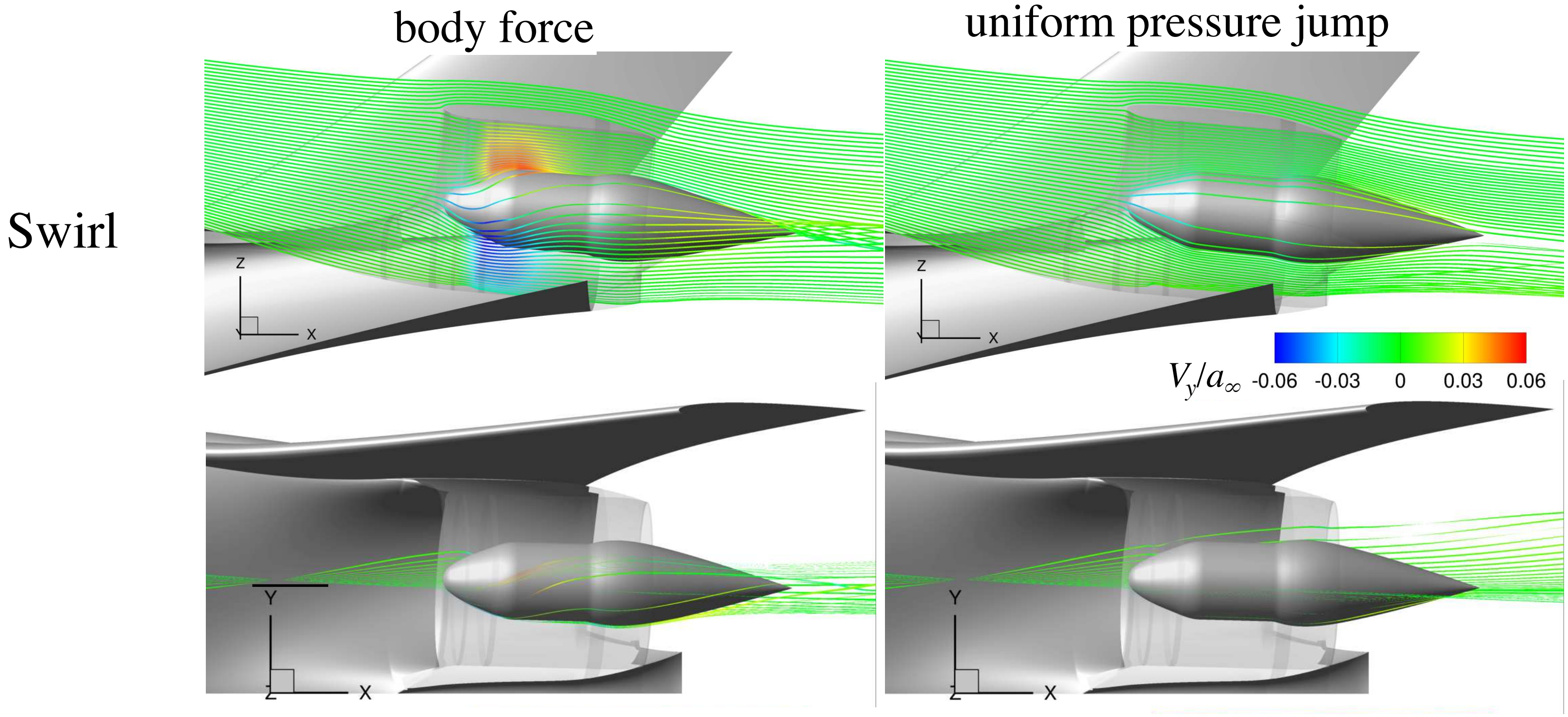

TF8000 propulsor on D8 -- Results

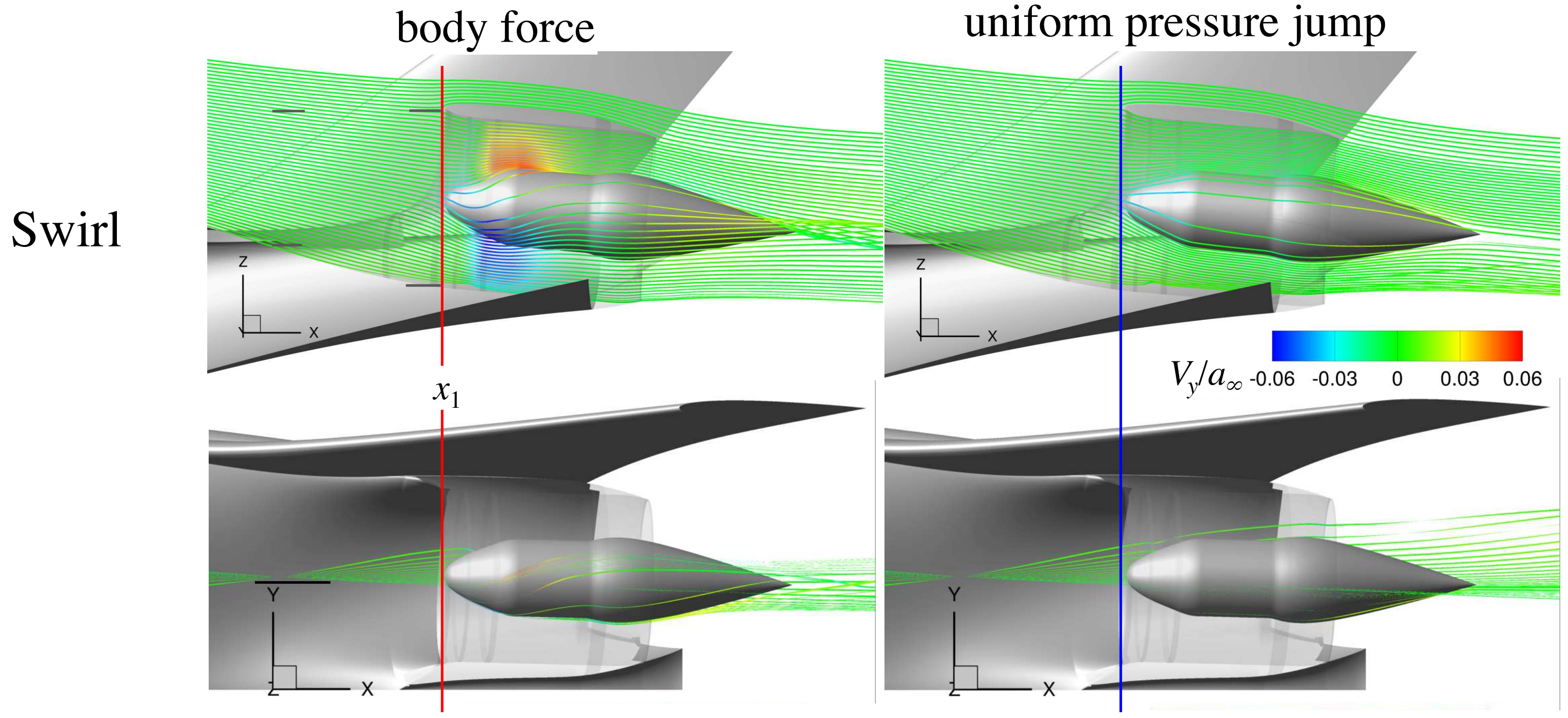

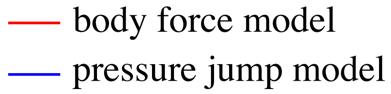

TF8000 propulsor on D8 -- Results

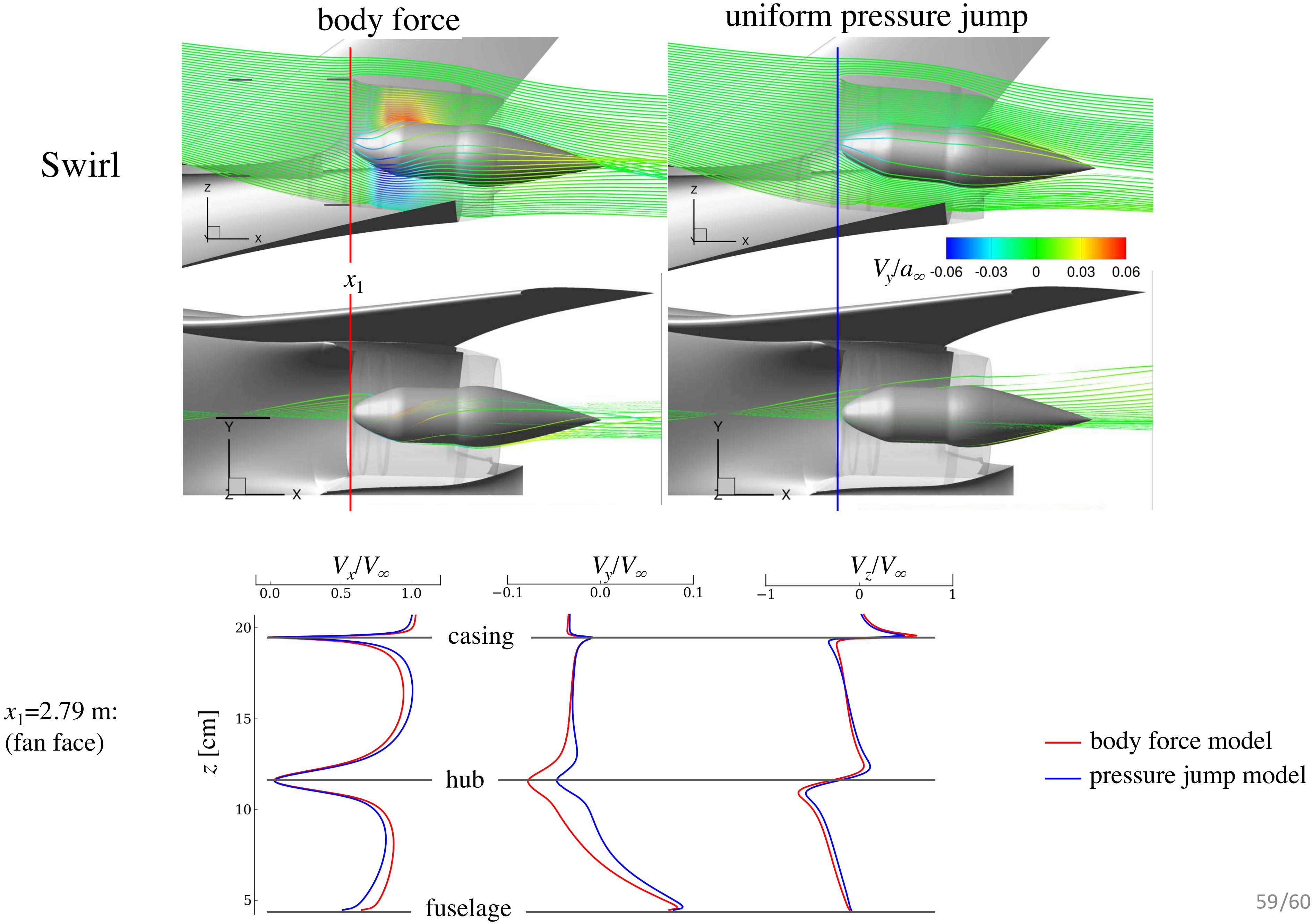

TF8000 propulsor on D8 -- Results

body force

uniform pressure jump

Swirl

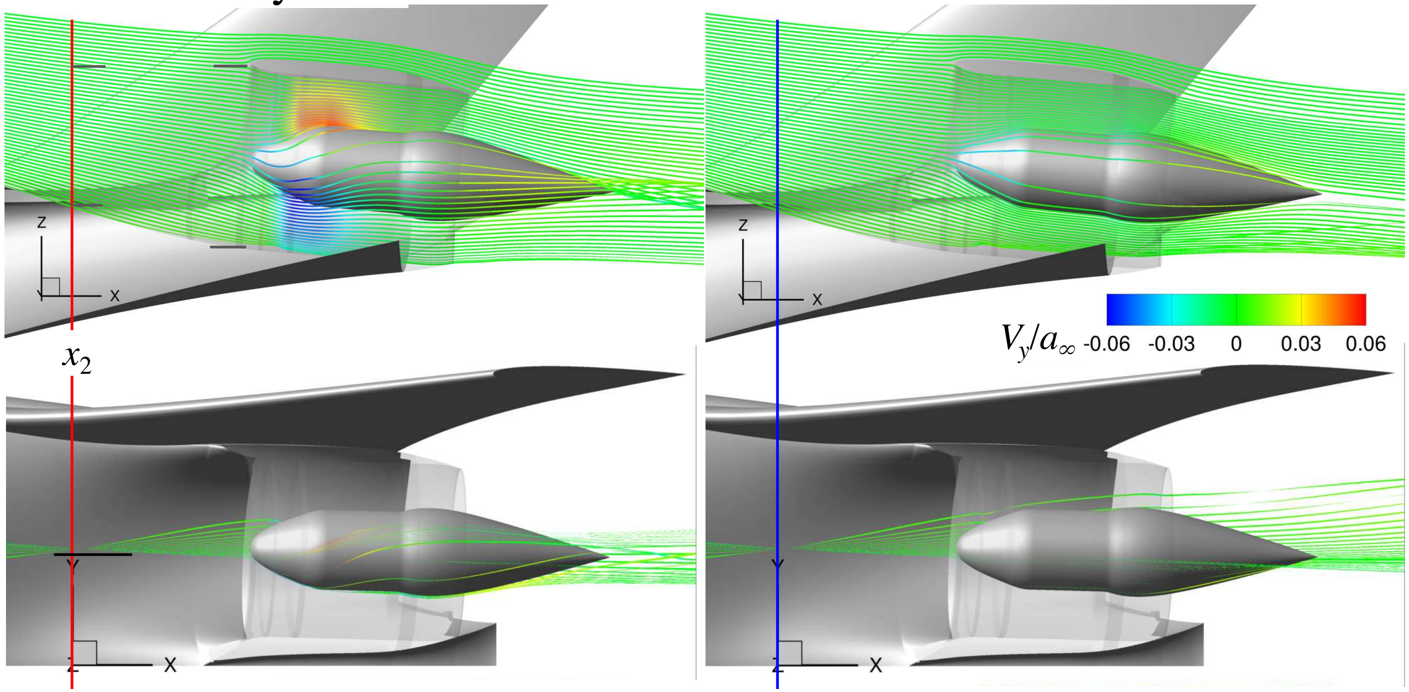

x_2=2.67 m:
(0.88d upstream)

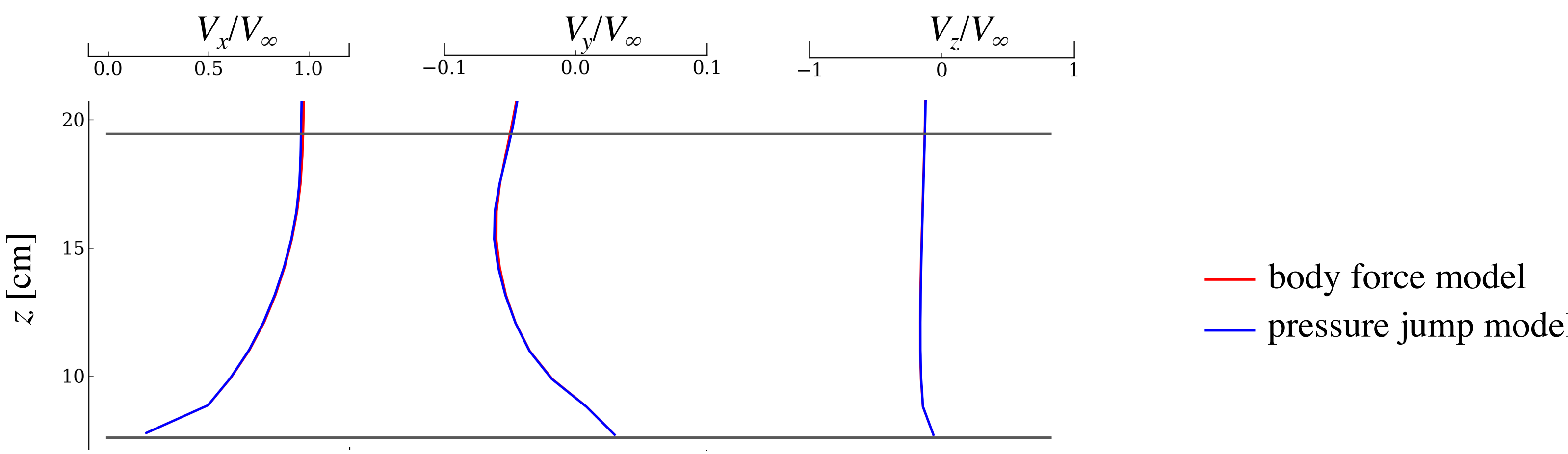

Summary & Discussion

- A body force model with blade loading by Hall et al. was successfully implemented in the Overflow solver.
- Generation of grids and blade orientation metrics were automated.
- The model predicted integrated quantities within a few percent on SDT with R4 rotor blades.
- The body force model provided detailed insights on the buildup of mechanical power throughout the propulsor.
- Demonstrated the need for an experimental data set on an isolated BLI fan.
- Further work would include adding compressibility, blade blockage and endwall corrections into the model.
- Further work would also include implementing propulsor models of various fidelities to assess the modeling fidelity sufficient for a given modeling goal.

Acknowledgements

- Dr. David K. Hall of the MIT Gas Turbine Laboratory provided a description of the source term computation algorithm.

- Dr. Edmane Envia of NASA Glenn Research Center provided the SDT aerodynamic data and geometry definition files.

- NASA Advanced Air Transport Technology (AATT) project provided the funding for this work.

- NASA Advanced Supercomputing (NAS) Division at NASA Ames Research Center provided computing resources.